Vapor pressure deficit helps explain biogenic volatile organic compound fluxes from the forest floor and canopy of a temperate deciduous forest

Paul C. Stoy[1,2,3,4], Amy M. Trowbridge[3,4,5], Mario B. Siqueira[6], Livia Souza Freire[7], Richard P. Phillips[8], Luke Jacobs[8], Susanne Wiesner[1,2], Russell K. Monson[9], Kimberly A. Novick[10]

[1]Department of Biological Systems Engineering, University of Wisconsin – Madison, Madison, WI, USA

[2]Department of Atmospheric and Oceanic Sciences, University of Wisconsin – Madison, Madison, WI, USA

[3]Department of Forest and Wildlife Ecology, University of Wisconsin – Madison, Madison, WI, USA

[4]Department of Land Resources and Environmental Sciences, Montana State University, Bozeman, MT, USA

[5]Department of Entomology, University of Wisconsin – Madison, Madison, WI, USA

[6]Department of Mechanical Engineering, Universidade de Brasília, Brasília, Brazil

[7] Instituto de Ciências Matemáticas e de Computação, Universidade de São Paulo, São Carlos, Brazil

[8]Department of Biology, Indiana University, Bloomington, IN, USA

[9]Department of Ecology and Evolutionary Biology, University of Colorado, Boulder, CO, USA

[10]Paul H. O'Neill School of Public and Environmental Affairs, Indiana University, Bloomington, IN, USA

Author Contributions: PCS, AMT, and RPP conceived of and designed the experiment and wrote the manuscript with input from all coauthors. MBS and LSF performed inverse modeling experiments, LJ and AMT made BVOC measurements, and KAN made tower micrometeorological measurements. SW created visual interpretations of the experimental setup and RPP and RKM assisted with data interpretation.

Abstract

Biogenic volatile organic compounds (BVOCs) play critical roles in ecological and earth-system processes. Ecosystem BVOC models rarely include soil and litter fluxes and their accuracy is often challenged by BVOC dynamics during periods of rapid ecosystem change like spring leaf out. We measured BVOC concentrations within the air space of a mixed deciduous forest and used a hybrid Lagrangian/Eulerian canopy transport model to estimate BVOC flux from the forest floor, canopy, and whole ecosystem during spring. Canopy flux measurements were dominated by a large methanol source and small isoprene source during the leaf-out period, consistent with past measurements of leaf ontogeny and theory, and indicative of a BVOC flux situation rarely used in emissions model testing. The contribution of the forest floor to whole-ecosystem BVOC flux is conditional on the compound of interest and is often non-trivial. We created linear models of forest floor, canopy, and whole-ecosystem flux for each study compound and used information criteria-based model selection to find the simplest model with the best fit. Most published BVOC flux models do not include vapor pressure deficit (VPD), but it entered the best canopy, forest floor, and whole-ecosystem BVOC flux model more than any other study variable in the present study. Since VPD is predicted to increase in the future, future studies should investigate how it contributes to BVOC flux through biophysical mechanisms like evaporative demand, leaf temperature and stomatal function.

Keywords: inverse model, isoprene, methanol, monoterpenes, proton transfer reaction mass spectroscopy

Introduction

Ecosystems are dynamic sources and sinks of biogenic volatile organic compounds (BVOCs), which play important roles in plant defense (Yuan et al. 2009; Junker and Tholl 2013), ecological signaling (Schiestl 2010; Holopainen and Blande 2012), oxidation chemistry, and atmospheric particle formation and growth (Fuentes et al. 2000, 2016; Kulmala et al. 2013; Faiola et al. 2014). BVOCs are also important in ecosystem and global carbon budgets. Their total global emission is on the order of 0.76 Pg C yr^{-1} (Sindelarova et al. 2014), nearly a quarter of the size of the net land carbon sink (Friedlingstein et al. 2019), and BVOC flux can comprise up to 10% of photosynthetic carbon uptake at the ecosystem scale (Peñuelas and Llusià 2003). These emissions, however, are dynamic and respond to continued shifts in land use, climate, and atmospheric chemistry (Peñuelas and Staudt 2010; Calfapietra et al. 2013; Hantson et al. 2017). It is thus critical to identify primary drivers contributing to ecosystem BVOC fluxes to better understand BVOC dynamics in a changing world.

Most ecosystem BVOC emissions arise from plant foliage (Figure 1) (Guenther 1997), particularly via plant stomata (Fall and Monson 1992), with important additional sources from leaf litter (Leff and Fierer 2008; Gray et al. 2010, 2014; Aaltonen et al. 2011). Dynamic source/sink behavior is also observed within the soil itself (Cleveland and Yavitt 1997; Insam and Seewald 2010; Bachy et al., 2016; Tang et al. 2019; Rinnan and Albers 2020). For example, in forests, soil BVOC flux results from belowground dynamics including the functioning of roots (Kreuzwieser and Rennenberg 2013; Gray et al. 2014) and their mycorrhizal associations (Trowbridge et al. 2020), which can subsequently alter the composition of the microbial communities that give rise to BVOCs (McBride et al. 2020). It is unclear if soils and litter make a sufficient contribution to total ecosystem BVOC flux to warrant inclusion in ecosystem models (Asensio et al. 2007), though recent studies indicate that they likely do (e.g. Bachy et al., 2016; Mäki et al. 2019). Aboveground

47 BVOC sinks include reactions with oxidative species within the plant canopy (Carter 1994;
48 Fuentes et al. 2007), dry deposition (Guenther 2015) and, critically, uptake by plant stomata such
49 that stomatal BVOC exchange should be treated as bi-directional (Niinemets et al. 2014) (Figure
50 1). Despite our recognition of complex interactions among BVOC emissions drivers, ecosystem
51 BVOC flux models tend to focus on emissions from just the plant canopy, rather than including
52 soils and leaf litter (Baldocchi et al. 1999; Niinemets et al. 2013; Guenther 2015), and they are
53 seldom challenged with observations from a broad set of ecosystem components. This study was
54 aimed at enhancing our understanding of ecosystem BVOC emission modeling with regard to soil
55 and litter processes and model inputs.

56 Models of ecosystem BVOC exchange are also challenged by plant phenology and
57 seasonality (Holzinger et al. 2006). These include emission bursts during periods of new foliage
58 growth (Aalto et al. 2014, 2015) that may be due to the direct exposure of plant resin to the
59 atmosphere (Eller et al. 2013), other aspects of plant-water relations like xylem refilling
60 (Vanhatalo et al. 2015), or the production or methanol and acetone during leaf ontogeny
61 (MacDonald and Fall 1993a; Nemecek-Marshall et al. 1995). These plant-associated fluxes are
62 controlled by a complex interplay among environmental and biological variables, including
63 intrinsic cellular processes as well as extrinsic factors such as air temperature, solar radiation, and
64 soil moisture (Monson et al. 1995; Guenther et al. 2012). Our knowledge about the interactions
65 among plant processes and the environment, however, is continually increasing and has progressed
66 since the creation of the current generation of ecosystem BVOC emission models.

67 Model development typically lags behind empirical discovery, making it likely that there
68 are additional intrinsic and extrinsic variables that need to be added to existing models. These
69 variables might include the vapor pressure deficit (VPD) which represents atmospheric demand

for water and is critical for plant canopy conductance (Novick et al. 2016), wind speed and canopy roughness, which influence canopy aerodynamic conductance and canopy air-space venting (Bohrer et al. 2009), the diffuse fraction of solar radiation, which can penetrate the plant canopy more efficiently than the direct beam to impact the radiative environment of the subcanopy (Oliphant and Stoy 2018; Moon et al. 2020), and the surface (skin) temperature, which may provide a more accurate description of the temperature at which biological processes occur compared to air temperature (Still et al. 2014; Pau et al. 2018). In addition to the emerging importance of soil and litter processes to accurately predict ecosystem BVOC fluxes, there is a need for studies that take a step back from the current form of emissions models and offer a fresh perspective of the relationships among model logic and existing knowledge of canopy and plant ecophysiological processes.

To study the dynamics of BVOC flux during the leaf-out period and investigate micrometeorological and vegetative controls necessary to explain their dynamics, we measured BVOC concentrations within a mixed deciduous canopy and estimated source and sink areas and fluxes using a hybrid Lagrangian/Eulerian canopy transport model. The transport model incorporated BVOC concentration measurements from a unique logarithmic canopy profiling system with a higher density of observations from lower in the canopy airspace, compared to past studies, which allowed us to isolate the contribution of the forest floor to ecosystem-scale BVOC exchange. The biotic diversity of species and traits in mixed forests creates additional challenges to understanding controls over sources and sinks of BVOCs (Kaharabata et al. 1999) and we included analyses of wind direction to understand if flux source area was important to describe efflux in the study forest. Finally, models of BVOC flux are increasingly cognizant of compounds that make a minor contribution to mass flux (Guenther et al. 2012) but may play disproportionate

roles in ecological interactions and atmospheric chemistry (Goldstein and Galbally 2007; Clavijo McCormick et al. 2014). We took care to not exclude an analysis of these minor compounds by exploring their relationship with BVOC compounds that comprise a larger proportion of total BVOC flux.

Methods

Study site

Measurements were made in the Morgan-Monroe State Forest in south-central Indiana, USA, at 39° 190' N, 86° 250' W on and around a long-running Ameriflux eddy covariance tower (site code US-MMS, Schmid 2000). The study site is an approximately 80-year-old mixed hardwood forest with trees that associate with ectomycorrhizal fungi (ECM) including shagbark and pignut hickory (*Carya ovata* and *C. glabra*), red and white oak (*Quercus rubra* and *Q. alba*), and American beech (*Fagus grandifolia*), and those that associate with arbuscular mycorrhizae (AM) including tulip poplar (*Liriodendron tulipifera*), sugar maple (*Acer saccharum*), and sassafras (*Sassafras albidum*). Seedlings and the isoprene-emitting spicebush (*Lindera benzoin*) are found in the understory. The mean canopy height in the vicinity of the tower was 27 m when measurements were made. Please see Brzostek et al. (2015) for additional site details.

Micrometeorological measurements

The US-MMS eddy covariance tower includes a full suite of micrometeorological measurements including: eddy covariance systems comprising CSAT3 (Campbell Scientific, Logan, UT) sonic anemometers and LI-7000 closed path infrared gas analyzers (LICOR, Inc., Lincoln, NE) at 46 m, 34 m, and 2 m above the forest floor; HMP35C air temperature/relative humidity measurements (Vaisala, Vantaa, Finland) at the same heights; a CNR-1 four-component radiometer (Kipp and

Zonen, Delft, The Netherlands) at 46 m; and CS615/6 (Campbell Scientific) soil moisture sensors and soil temperature measurements at 10 cm depths to bedrock. We use direct and diffuse photosynthetically active photon flux density (PPFD), measured by a BF3 sunshine sensor (Delta-T Devices, Cambridge, UK) to describe BVOC responses to the light environment.

Proton transfer reaction-mass spectroscopy

BVOC measurements were made using a proton transfer reaction-mass spectrometer (PTR-MS; Ionicon Analytic, Innsbruck, Austria) housed in an air-conditioned research building adjacent to the US-MMS tower. We selectively analyzed 49 different mass/charge (m/z) ratios following previous work on compounds identified in ambient air (Gouw et al. 2007; Blake et al. 2009; Ellis and Mayhew 2013) (Table S1). We focus on key compounds for which we have calibration standards, namely formaldehyde, methanol, acetonitrile, acetaldehyde, acetone, dimethyl sulfide (DMS), isoprene, methyl vinyl ketone (MVK), methacrolein, methyl ethyl ketone (MEK), benzene, toluene, C8 aromatics, C9 aromatics, and monoterpenes (Table S1). Concentrations of the fragments of isoprene and monoterpene (m/z 41 and m/z 81) were calculated using a theoretical transmission curve created for the PTR-MS instrument. The concentrations of the fragments were then added to the concentration measurements of the compounds calculated using calibration. Calibrations were performed prior to each measurement campaign using a multi-component calibration mix (±5% confirmed by the manufacturer using GC-MS) stored in nitrogen gas (Apel-Riemer Environmental, Inc.). We studied the time series of the normalized mass-to-charge (m/z) ratios of compounds for which calibration standards were not available to see if they follow similar patterns to compounds with calibration standards.

The PTR-MS drift tube pressure (p) was set at 2.1 mbar and temperature (T) to 333.15 K with a drift field of 600 V. The parent ion signal was set to ~ 1×10^6 counts per second. The

protonated oxygen to primary ion count (O_2^+:H_3O^+) ratio was < 3.5%. The volume mixing ratio (VMR, ppbv) of calibrated compounds was calculated by dividing its m/z by its calibration coefficient calculated using a linear fit. To calculate concentrations using the transmission factor approach, the volume mixing ratio VMR of each compound was calculated following (Ellis and Mayhew 2013):

$$VMR = \frac{i(MH^+)\times 10^9}{i(H_3O^+)ktN_d} \quad (1)$$

where $i(MH^+)$is the protonated compound of interest divided by its transmission factor, $i(H_3O^+)$ is the primary ion count divided by its transmission factor and multiplied by 500, k is the rate coefficient, t is reaction time, and the total number density of the gas in the drift tube, N_d, is:

$$N_d = \frac{pA_N}{RT} \quad (2)$$

where p is in Pa, A_N is Avogadro's number, and R is the ideal gas law constant (8.3145 m^3 Pa mol^{-1} K^{-1}). We note that this approach incurs uncertainty on the order of 2% by using 500 rather than 489.56 for the ion count multiplier.

Canopy profile measurements

The canopy BVOC profile measurement campaign took place from May 8 to May 25, 2015 with a 77-minute missing measurement period during maintenance on May 12. During sampling, the inlet of the PTR-MS was attached to the canopy profiling system with measurements at 0.25 m, 0.5 m, 1 m, 2 m, 4 m, 8 m, 16 m, and 32 m (i.e. 2^{-2} to 2^5 m). Measurements were made every 10.45 seconds. The first three and last PTR-MS measurements at each level were discarded to ensure that the sample air originated from the measurement height at time of measurement. The remaining observations at each level were then used to calculate a mean concentration of each of the study compounds.

Canopy flux estimation

Estimating the net flux of a scalar (here, BVOCs) from canopy profile observations requires a model that can compute spatially-distributed scalar sources from time-distributed concentration measurements, known as the 'inverse problem' (Raupach 1989a). The challenge is to infer the source and sink (S) dynamics of a scalar as a function of height (z) from measurements of the scalar concentration (c) at different heights in the canopy across time (t) which are coupled by the principle of continuity and the scalar concentration budget equation (see Monson and Baldocchi 2014). The time- and horizontally-averaged steady-state scalar conservation equation for planar homogeneous high Reynolds and Peclet numbers flow (i.e. neglecting molecular diffusion, (Finnigan 1985; Raupach 1988) is given by:

$$\frac{\partial <\bar{c}>}{\partial t} = 0 = -\frac{\partial <\overline{w'c'}>}{\partial z} + S \quad (3)$$

where w is vertical velocity, primes are fluctuations from time averages (represented by overbars), and the angle bracket denotes horizontal averaging as discussed in Raupach and Shaw (1982), such that $< \overline{w'c'} >$ represents the turbulent vertical flux of a scalar.

Early approaches used 'K-theory', which assumes that scalar fluxes and, consequently, S (Eq. 3), are related to scalar gradients through an eddy diffusivity coefficient within the plant canopy, which can vary with height. However, the dynamics of turbulence within plant canopies, including counter-gradient fluxes, often result in a situation where K-theory becomes unreliable (Denmead and Bradley 1985). Whereas some approaches have improved models for eddy diffusivity to account for these shortcomings (Freire et al. 2017), here we adopt the 'hybrid' approach of Siqueira et al. (2000) that combines the two dominant approaches designed to overcome the limitations of K-theory: inverse Lagrangian localized near-field (LNF) theory (Raupach 1989a, b) and high-order Eulerian closure models (Katul and Albertson 1999).

In brief, the hybrid approach acknowledges that LNF theory assumes normally-distributed vertical velocity statistics, but also recognizes that non-Gaussian ejection-sweep cycles frequently drive mass transport within tall plant canopies (Figure 1), and that pure Eulerian formulations are sensitive to uncertainties in the measurement of c due to a limited scope for replication in the inversion of S from c (Siqueira et al. 2000). To overcome these limitations, Siqueira et al. (2000) proposed a model that retains the concept of the inverse Lagrangian approach, which grants the model the desired robustness to measurement errors but using the Eulerian frame of reference to estimate the elements of the dispersion matrix, thus mechanistically accounting for vertical-velocity skewness effects in scalar transport.

The procedure consists of dividing the canopy into multiple layers (Figure 1). The task then becomes to find the combination of the canopy layer source and sink strengths (i.e. S) that best recover the measured mean scalar concentration profile. In an inverse sense, the dispersion matrix is constructed by dividing the canopy into layers of unit source strength and then calculating the expected mean concentration profiles from each layer individually using the scalar-flux budget equation (Eq. 3), which is re-arranged to provide a differential equation for scalar concentration (see Supplemental Material). Neglecting buoyancy, scalar drag and waving source terms, the time and horizontally-averaged steady-state equation can be written as a second-order ordinary differential equation (ODE) for scalar concentration as a function of height (Siqueira et al. 2000):

$$M_1(z)\ \frac{\partial^2 <\bar{c}>}{\partial z^2} + M_2(z)\ \frac{\partial <\bar{c}>}{\partial z} = M_3(z) \qquad (4)$$

where c is the scalar concentration function of height. The coefficients $M_{1,2,3}$ are functions of scalar flux and turbulent velocity statistics. The profiles of velocity statistics, when normalized by friction velocity (u*) at a reference height, becomes a function only of leaf-area-density vertical

distribution (LAD), provided for MMSF by Oliphant et al. (2006) (Figure 1) and can be obtained by a second-order closure model for turbulent flow. Here, we used the model described in Siqueira et al. (2012), who explicitly solved an equation for turbulent-kinetic-energy dissipation, required for the *M*-coefficients.

Equation (4) is not closed because it requires the scalar fluxes, which can be obtained by Eq (3) given source distribution is known. With a prescribed source, as is the case for dispersion-matrix construction, the scalar budget equation (Eq. 3) can be integrated to provide the flux used in the *M*-coefficients. Furthermore, with proper boundary condition, Eq. (4) can be numerically solved (here we used a finite-volume technique) to give the vertical profile of $< \bar{c} >$.

Next, the dispersion matrix is computed from

$$D_{ij} = \frac{<\bar{c}>_i - \bar{C}_R}{s\Delta z_j} \quad (5)$$

where, $< \bar{c} >_i$ represents the concentration at the measurement height *i* (*i*=1,2,…,*n*) resulting from the source layer *j* (*j*=1,2,…,*m*), calculated using Eq. (3) and (4), and $\bar{C}_R$ is the concentration at a reference height. We adopted the last measurement height (32 m) as the reference, which was used as the boundary condition for Eq. (4). D_{ij} are the elements of the (*n* by *m*) dispersion matrix, *s* is an assumed unitary source strength, and Δz_j is the source layer thickness. Once the dispersion matrix is determined, the source strengths S_j can be readily computed if *m* = *n*:

$$\bar{C}_{i,m} - \bar{C}_R = \sum_{j=1}^{m} D_{ij} S_j \Delta z_j \quad (6)$$

where $\bar{C}_{i,m}$, contrary to (5), are the time-averaged concentrations at height *i*. However, this would make estimated source sensitive to measurement errors (Raupach, 1989a). To avoid such instability, redundant concentration measurements are necessary (i.e. *n* > *m*), such that the system

becomes over-determined. As shown by Raupach (1989a), such redundancy reduces (6) to a regression problem with the source strengths calculated by a least-squares approach:

$$\sum_{k=1}^{m} A_{jk} S_k = B_j \quad (j=1,..,m) \tag{7}$$

where:

$$A_{jk} = \sum_{i=1}^{n} D_{ij} \Delta z_j D_{ik} \Delta z_k \tag{8}$$

and

$$B_j = \sum_{i=1}^{n} (C_i - C_R) D_{ij} \Delta z_j \tag{9}$$

The above regression procedure addresses the limited-sampling problem inherent in pure Eulerian frameworks. However, such an approach, when applied to a limited sample size, retains high variance among redundant source estimates. To improve assessment of retrieved source values and their associated variances, an additional smoothness constraint was imposed on (7) and (8) using the Weighted Measures of Length procedure (Menke, 2018; Siqueira et al. 2000).

Modeling analysis

We created linear models of the forest floor, canopy, and ecosystem flux of each studied BVOC compound (Table 1) as a function of multiple micrometeorological variables and the surface-atmosphere flux of carbon, water, and heat, fit using maximum likelihood. We discriminated amongst the models by calculating the Akaike's Information Criterion for each with the assistance of the *dredge* function in the MuMIn package (Bartoń, 2020) using R version 4.0.0 (R Core Team, 2020) and selecting the model with the lowest AIC as the most parsimonious. The goal of the modeling analysis is to determine which variables should not be excluded for understanding

247 micrometeorological and canopy controls over BVOC flux rather than creating models of the flux
248 of 14 compounds from three sources during the leaf-out period of a mixed deciduous forest. The
249 micrometeorological variables used to create the models – in addition to those listed above –
250 include below canopy and diffuse PPFD (as a surrogate for incident solar radiation), soil
251 temperature and moisture, VPD, wind speed and direction as a surrogate for source area within the
252 diverse forest canopy, and canopy and forest floor surface (skin) temperature calculated from
253 outgoing longwave radiation measurements using the Stefan-Boltzmann Law and assuming a
254 canopy and forest floor emissivity of 0.98 (Jin and Liang 2006).
255
256 **Results**
257 *Meteorology*
258 The May 8 – 26, 2015 measurement period was characterized by alternating (relatively) warm and
259 cool air temperatures (Figure 2A). Most precipitation events occurring during the first half of the
260 measurement period (Figure 2A) and variability in PPFD resulted in warm/mostly sunny (May 8-
261 11, 15, 23-25), warm/cloudy (May 16-18, 26), cool/mostly sunny (May 12-14, 19, 22) and
262 cool/cloudy (May 20-21) periods (Figure 2A and 2B). VPD was relatively high (> 20 hPa) on May
263 8 when measurements began and during the latter part of the measurement period (May 24-25,
264 Figure 2C). Prevailing winds arrived largely from the SSW (Figure 2D, S1A and S1B) with a peak
265 distribution at 190 degrees at 46 m and 200 degrees at 34 m. Subcanopy wind speed was dominated
266 by flows from the SW with little contribution from the SE (Figure 2D and S1C). Plant area index
267 increased throughout the May 2015 measurement period from 3.4 m^2 m^{-2} to 4.7 m^2 m^{-2} (Figure 3).
268 *BVOC concentrations within the canopy*

Methanol had the highest mean (± s.d.) concentration across all measurement heights at 12.7 ± 6.5 ppbv (Table 1). Within-canopy mean BVOC concentrations of the key compounds methanol, isoprene, and monoterpenes were relatively high during the earlier part of the measurement period (Figure 4), then declined and increased again on May 15 during a warm period after a small rain event. Canopy BVOC concentrations rose again during the warm and sunny period of May 23-25. Notably, methanol, isoprene, and monoterpene concentrations were often higher in the overstory at 16 m during May 8-9 and May 13 and isoprene and monoterpene concentrations were often higher near the soil surface and subcanopy at 0.25 m and 0.5 m from May 15-25 (Figure 4), implying different sinks and sources within the canopy volume.

The time series for most key compounds exhibited characteristic concentration profiles as a function of time of day and canopy height with elevated concentrations in the afternoon within the canopy and near the forest floor (Figure 5) except methanol, which had an early morning peak throughout the canopy volume, on average, and formaldehyde which had a peak in the lower forest canopy in the afternoon. The mass-to-charge ratios of most of the 49 compounds studied also exhibited a characteristic pattern with higher values within and above the canopy and in the afternoon (Figure S2) noting that many compounds were close to the signal-to-noise ratios as evidenced by the striping pattern in the time / height concentration plots. Some compounds exhibited time / height concentration dynamics that were unique compared to other profiles (e.g. m/z 32, Figure S2).

Modeled BVOC fluxes, sources, and sinks

Models of the second and third moments of the vertical velocity normalized by u^* matched observations well on average (Figure S3). Modeled BVOC concentrations likewise tended to match measurements well with the exception of the lower canopy where modeled values were

292 frequently lower than measurements (Figure 6) due likely in part to challenges in modeling
293 turbulence near surfaces (the boundary layer effect) and challenges in redistributing parcels toward
294 the surface in Lagrangian approaches. Forest floor BVOC source strength may be underestimated
295 and/or sink strength overestimated as a consequence and results are subject to this uncertainty.

296 Most BVOC compounds exhibited a relatively large net efflux to the atmosphere from the
297 plant canopy from the beginning of the measurement period starting at mid-day on May 8 until
298 mid-day on May 9 (Figure 7) that resulted from (relatively) high BVOC concentrations in the
299 overstory at 16 m during the first day of measurements (e.g. Figure 4). There was a subsequent net
300 uptake of most studied BVOC compounds from May 9 until May 12 during a period when mid-
301 day temperature decreased from nearly 28 °C to less than 16 °C with cloudier conditions (Figure
302 2 and 7). This was followed by another net efflux of most BVOC compounds from mid-day on
303 May 12 until mid-day on May 13 during a sunnier period (Figure 2 and 7). Afterward, net BVOC
304 flux from the overstory tended to be minor for some compounds (e.g. methanol) or exhibit net
305 uptake for others (e.g. isoprene). The forest floor was a net cumulative sink of BVOCs across most
306 of the measurement period, which tended to buffer net canopy fluxes such that the net ecosystem
307 source was smaller than net canopy source alone (Figure 7), keeping in mind that the forest floor
308 sink strength is likely underestimated (Figure 6). There was an increase in forest floor BVOC
309 efflux during the last two days of measurements from mid-day on May 23 until mid-day on May
310 25 (Figure 7) during a warmer period (Figure 2A) when subcanopy and above-canopy wind
311 direction was decoupled (Figure 2D) as the forest canopy approached closure (Figure 3). As a
312 result of this similar behavior across time, the ecosystem fluxes of all study compounds were
313 significantly related to each other and the flux of one compound explained up to 81% of the
314 variability of other compounds (Figures S4 and S5). The canopy overstory was a net source of

BVOCs and the canopy air space below it was on average a net sink with the exception of the understory vegetation which was a notable source of BVOCs, especially toward the latter part of the measurement period as demonstrated for the key compounds methanol, isoprene, and monoterpenes (Figure 8).

Ecosystem models

Leaf area index (LAI) and VPD entered the most parsimonious ecosystem, canopy, and forest floor BVOC flux model on 39 of 42 and 41 of 42 instances, respectively (Table 2) and had the strongest correlation with the key study species methanol, isoprene, and monoterpenes (Figure 9). Air (canopy) temperature entered the most parsimonious model on 31 (30) of 42 instances and soil temperature and the diffuse fraction of photosynthetically active radiation entered the most parsimonious model for forest floor flux on 12 of 14 instances. Below-canopy radiation was never an important input, but wind speed and direction often were.

Discussion

Ecosystem BVOC efflux

We observed a relatively large BVOC efflux from the canopy during the early part of the May measurement period (May 8-9), especially at 16 m (Figures 4 and 8). This height roughly aligns with the canopy layer of maximum leaf-area density located vertically near the middle of the foliated portion of the canopy (Figure 1). The observation of this early-spring efflux occurs during the period of rapid leaf expansion, in this case during the time that leaves expanded from approximately 70% to 95% of full expansion area (Figure 3). Methanol fluxes were at least an order of magnitude higher than all other BVOC emissions, including isoprene, which normally dominates emissions in eastern US deciduous forests (Geron et al. 1994; Isebrands et al. 1999). It

is likely that the high methanol fluxes that we observed, and the fact that isoprene emission rates were much lower, are associated with the physiological maturation of leaves. Methanol is known to be formed at high rates during leaf expansion as a product of pectin demethylation during cell-wall loosening (Levy and Staehelin 1992; MacDonald and Fall 1993b; Galbally and Kirstine 2002). High methanol emissions have been observed during the early spring leaf-out period from other mixed forests in the north-central US (Karl et al. 2002; McKinney et al. 2011) and boreal forests (Aalto et al. 2014; Schallhart et al. 2018). At the same time, isoprene is known to be emitted at low to negligible rates early during leaf expansion and is only fully activated as leaves near full expansion (Grinspoon et al. 1991), or after treatment by relatively high accumulated temperature (Monson et al. 1994). Fluxes and atmospheric concentrations of monoterpenes were relatively low (Table 1, Figure 7) likely due to the lack of coniferous species in the forest canopy. The combination of relatively high methanol fluxes and relatively low terpenoid fluxes represents a chemical-flux landscape seldom studied with regard to model testing and provided us with an opportunity to challenge the coupling between modeled emissions and climatic drivers in a novel ecosystem context (see also Aalto et al. 2014).

The estimated rate of canopy isoprene emissions at its peak in early May was approximately 10% of the rate previously measured in eastern US forests (Goldstein et al. 1998; Baldocchi et al. 1999). Of course, comparisons of isoprene emissions rates among sites will depend on the fraction of trees at each site that emit isoprene. However, the Morgan-Monroe forest has a relatively high representation of oaks, which are high isoprene emitters, and there is no reason to suspect that such low isoprene emission rates, compared to other sites, are due to forest species composition. Rather, it is more consistent with suppressed emission rates due to leaf ontogenetic effects, as described above. Even with low basal emission capacities, however, isoprene emissions responded to

changes in seasonal weather conditions. Isoprene emissions reached relatively high rates during the warm, cloudless period of May 8-12, consistent with its high sensitivity to PPFD and leaf temperature, but the cold, cloudy periods between May 12-16 and again between May 19-22, appear to have caused a persistent decrease, consistent with past studies that have shown a close coupling of isoprene emissions to prevailing weather periods and photosynthesis, and a lag in recovery to high emission rates following short periods of cool, cloudy weather (Sharkey et al. 1999). On May 12, during a period of relatively high solar radiation, the prevailing wind direction switched from its normal SSW flow to become progressively more northerly, causing the profiling system to measure different area of the forest (Figure 2B and 2D). This shift may have contributed to the noticeable dip in emissions of all BVOCs, but especially for isoprene and methanol, on May 12.

BVOC sources dominated the observed total canopy flux, as forest floor sinks were small during this part of the growing season (Figure 7). Overall, the emission profile for this springtime campaign is skewed toward high methanol emissions, but still responsive to climate variation, especially temperature, with regard to terpenoid emissions. This creates a novel set of data for testing emissions models because there is evidence of clear responses to the conventional climate drivers of temperature and PPFD, but with the added early-season condition of high methanol emissions due to phenological drivers.

Forest floor BVOC efflux

The forest floor was a net sink of most study BVOCs during most of the measurement period (Figure 7) in agreement with the results of soil BVOC flux measurements from MMSF during the early growing season of the previous year (Trowbridge et al. 2020) and noting again that the forest

floor sink strength from profile measurements should be interpreted as an underestimate of the true flux (Figure 6). These observations align with numerous recent studies demonstrating that soils are often net sinks for BVOCs (Rinnan and Albers 2020; Trowbridge et al., 2020). Importantly, the role of the forest floor as a BVOC sink in the absence of fresh litter inputs during the leaf-out period buffered canopy BVOC flux during most of the measurement period such that whole-ecosystem BVOC flux was lower than canopy BVOC flux (Figure 7), but this effect varied by compound. Monoterpene flux from the forest floor was trivial (a fraction of a mmol m^{-2} over the study period) such that canopy and ecosystem effluxes were nearly identical (Figure 7) but the forest floor and canopy flux of compounds like acetonitrile were of similar orders of magnitude such that including forest floor flux is necessary to describe whole-ecosystem flux even if the magnitudes of the flux of these compounds are relatively small (Figure 7). These results suggest that the inclusion of the forest floor to whole-ecosystem BVOC flux is conditional on the compound of interest during the leaf out period. Notably, many minor compounds tended to be highly correlated to two of the calibrated compounds, DMS (Whelan and Rhew 2016) and acetaldehyde (Karl et al. 2002) (Table S1), that had non-trivial contributions of forest floor BVOC flux to ecosystem BVOC flux across most of the measurement period (Figure 7) suggesting that forest floor fluxes of minor compounds may likewise be a non-trivial proportion of their whole-ecosystem fluxx.

Ecosystem modeling

Air temperature and PPFD (as a surrogate of shortwave radiation) frequently entered the most parsimonious model of BVOC fluxes as anticipated (Table 2) and there was little evidence that alternate measurements of temperature or PPFD (e.g., skin temperature or diffuse fraction)

represented an improvement (Table 1): air and radiometric canopy temperatures entered the most parsimonious ecosystem, canopy, and forest floor models on the same number of instances but the latter is a more difficult measurement to make. These observations suggest – at least for the study ecosystem and measurement period – that the variability in canopy and forest floor temperature as well as below-canopy and diffuse radiation provide little new information to canopy and ecosystem BVOC models than simple air temperature and incident radiation at or near the top of the canopy (Guenther et al. 2006; Arneth et al. 2011). Likewise, radiometric forest floor temperature did not represent an improvement over soil temperature for forest floor BVOC flux modeling.

Atmospheric VPD, on the other hand, consistently entered the linear model with the lowest AIC score for canopy, forest floor, and whole-ecosystem BVOC flux models, and entered these models more than any other variable, including air temperature and PPFD (Table 2). This is perhaps an unexpected result given that nearly all flux modeling over the past three decades for isoprene and monoterpenes – the dominant compounds emitted from most forested ecosystems – has been founded on temperature and light as the dominant driving variables, and with good physiological justification (Monson et al. 2012). It is possible that the importance of VPD arises because of the diversity of BVOCs that we analyzed and the fact that several of them have low Henry's Law volatility coefficients that renders their flux susceptible to stomatal control. For the case of methanol, the BVOC emitted at highest rates during the spring campaign, it has long been known that leaf emission rates are determined by stomatal conductance dynamics (Nemecek-Marshall et al. 1995), or a combination of stomatal conductance and leaf temperature (Harley et al. 2007). The tendency for a BVOC compound to be controlled, or not, by stomatal conductance dynamics was explained using chemical theory by Niinemets and Reichstein (2003). Oxygenated BVOCs, such as methanol, acetone, acetaldehyde, MVK, formaldehyde and acetonitrile,

preferentially partition into the liquid phase of the leaf and are emitted in a pattern similar to that of water molecules, with significant modification by stomatal control. Hydrocarbon compounds, such as the terpenoids, partition preferentially into the gas phase of the leaf, and are not susceptible to stomatal control during steady-state emissions (also see Fall and Monson 1992). It is also worth noting that the canopy flux of oxygenated compounds, like methanol, are also highly susceptible to uptake into moisture films on canopy surfaces (Laffineur et al. 2012). This can cause the canopy to be a sink for these compounds, especially during the early morning and after rain events, when VPD would also be low. Between stomatal control over emissions at high VPD and uptake to the canopy at low VPD, a correlation between net emission rates and VPD dynamics in the modeling is likely explained (Figure 9). Thus, the tendency for VPD to control canopy BVOC emissions during the spring might result from it falling into the model for many of the oxygenated compounds that were observed.

It is surprising, however, that VPD emerged as a significant control in the modeling of nearly all compounds from all sources (Table 2). This means that it also influenced significant control over dynamics in several of the relatively hydrophobic terpenoids. It is not clear at this time as to how such control occurs. It could be due to the fact that there is a high degree of correlation between VPD and air temperature (Figure 9), and air temperature exerts such strong control over hydrocarbon emissions (due to their low boiling points). It is possible that the cross-correlation between VPD and temperature is causing VPD to appear as important in the Akaike's Information Criterion analysis. Ecosystem BVOC models tend to use soil moisture to simulate plant water stress (Guenther et al. 2012) and SWC entered many of the most parsimonious BVOC flux models even though it was not lower than 33% during the measurement period and therefore not likely to be limiting (Rodriguez-Iturbe et al. 2001) but it did not enter models as frequently as

VPD. Our results suggest that VPD is a logical variable to add to BVOC flux models and we recommend additional experiments to explore its role in BVOC flux at the ecosystem scale.

It is also important to note that wind speed and direction consistently entered models with the lowest AIC values, implying that the source area of the sampled air mass in the diverse study forest is important for describing BVOC flux (Table 2), as anticipated given the importance of source area for BVOC flux measurements (Guenther et al., 1996). LAI was also an important variable modeling BVOC flux as anticipated given its critical role in existing flux models (Guenther et al. 2006). It also entered all models of forest floor BVOC flux suggesting that it may be an effective surrogate of whole-ecosystem BVOC dynamics due to simultaneous belowground autotrophic activity. It is also important to note that $PPFD_{DIF}$ entered the most parsimonious forest floor flux model in most instances, but below-canopy radiation itself did not. These results are consistent with the notion that BVOC flux associated with photodegradation – known to be important to litter decomposition (Austin and Vivanco 2006) – played little role in forest floor BVOC flux but that the light environment below the canopy itself did (Moon et al. 2020). Fluxes of the study BVOC compounds were often highly correlated with each other (Figure 9 and S4, Table S1), as has been found in multiple other studies (Schade and Goldstein 2001), further lending confidence to the notion that BVOCs can be modeled categorically (Guenther et al. 2012). As a whole our modeling results point to the importance of the canopy light environment and evaporative demand for controlling BVOC flux in addition to the key variables included in models.

Conclusions

We coupled BVOC flux estimates from canopy profile observations and a canopy transport model. Modeled BVOC concentration tended to fit observations well with the exception of the lower canopy layers, suggesting that the modeled forest floor BVOC sink may be underestimated.

Observations demonstrate that the addition of VPD may be a logical approach for further improving BVOC model fit and that the contribution of the forest floor to whole ecosystem BVOC flux was either trivial or non-trivial depending on the compound of interest. The fluxes and concentration time series of many compounds were highly correlated, further lending strength to the idea that they can be modeled categorically. Future research should further explore the mechanisms by which VPD controls ecosystem BVOC flux and how the forest floor and canopy combine to create whole-ecosystem BVOC fluxes.

Data Availability

Eddy covariance and micrometeorological data are available at https://doi.org/10.17190/AMF/1246080 (Novick and Phillips (1999-). BVOC observations from the profiling system are available at https://figshare.com/articles/dataset/Biogenic_volatile_organic_compound_concentrations_from_a_vertical_profiling_system_in_a_mixed_deciduous_forest_in_Indiana_USA/12746273. BVOC fluxes are available at https://figshare.com/articles/dataset/Biogenic_volatile_organic_compound_fluxes_from_the_forest_floor_canopy_and_whole_ecosystem_in_a_mixed_deciduous_forest_in_Indiana_USA/12746384.

Acknowledgements

We wish to acknowledge the Indigenous Nations on whose ancestral lands and ceded territories the study took place and recognize that the infrastructure used for this project is built on Indigenous land. We recognize the myaamiki, Lënape, Bodwéwadmik, and saawanwa people as past, present,

and future caretakers of this land whose stewardship of the region was interrupted through their physical removal by the 1830 Indian Removal Act and through US Assimilation policies explicitly designed to eradicate Indigenous language and ways of being until the 1970s. This research was supported by the U.S. Department of Energy Office of Science (BER) (DE-SC0010845) and a National Science Foundation (NSF) Postdoctoral Research Fellowship in Biology (1309051). Long-term operation of the US-MMS flux tower is made possible with support from the AmeriFlux Management Project, administered by the Department of Energy's Lawrence Berkeley National Lab. We thank Tyler Roman, Dr. Berk Knighton, and Ern Trowbridge for logistical support, Aaron Bird Bear and colleagues for cultural knowledge, and Dr. Jeremy Kedzoria for statistical insight. PCS acknowledges support of the Alexander von Humboldt-Foundation, the National Science Foundation Division of Environmental Biology grant #1552976, and the University of Wisconsin – Madison. This manuscript is to be published as part of a Special Issue honoring the career of Russ Monson. We are grateful for his mentorship and decades of research on volatile organic compound fluxes that inspired the present analysis.

Conflict of Interest

The authors declare that they have no conflicts of interest.

References

Aalto J, Kolari P, Hari P, Kerminen V-M, Schiestl-Aalto P, Aaltonen H, Levula J, Siivola E, Kulmala M, Bäck J (2014) New foliage growth is a significant, unaccounted source for volatiles in boreal evergreen forests. Biogeosciences 11:1331–1344.

https://doi.org/10.5194/bg-11-1331-2014

Aalto J, Porcar-Castell A, Atherton J, Kolari P, Pohja T, Hari P, Nikinmaa E, Petäjä T, Bäck J (2015) Onset of photosynthesis in spring speeds up monoterpene synthesis and leads to emission bursts. Plant, Cell and Environment 38:2299–2312. https://doi.org/10.1111/pce.12550

Aaltonen H, Pumpanen J, Pihlatie M, Hakola H, Hellén H, Kulmala L, Vesala T, Bäck J (2011) Boreal pine forest floor biogenic volatile organic compound emissions peak in early summer and autumn. Agricultural and Forest Meteorology 151:682–691. https://doi.org/10.1016/j.agrformet.2010.12.010

Arneth A, Schurgers G, Lathiere J, Duhl T, Beerling DJ, Hewitt CN, Martin M, Guenther A (2011) Global terrestrial isoprene emission models: sensitivity to variability in climate and vegetation. Atmospheric Chemistry and Physics 11:8037–8052. https://doi.org/10.5194/acp-11-8037-2011

Asensio D, Penuelas J, Ogaya R, Llusia J (2007) Seasonal soil VOC exchange rates in a Mediterranean holm oak forest and their responses to drought conditions. Atmospheric Environment 41:2456–2466. https://doi.org/10.1016/j.atmosenv.2006.05.007

Austin AT, Vivanco L (2006) Plant litter decomposition in a semi-arid ecosystem controlled by photodegradation. Nature 442:555–558. https://doi.org/10.1038/nature05038

Bachy A, Aubinet M, Schoon N, Amelynck C, Bodson B, Moureaux C, Heinesch B (2016) Are BVOC exchanges in agricultural ecosystems overestimated? Insights from fluxes measured in a maize field over a whole growing season. Atmospheric Chemistry and Physics, 16:5343–

5356. https://doi.org/10.5194/acp-16-5343-2016

Baldocchi DD, Fuentes JD, Bowling DR, Turnipseed A, Monson RK (1999) Scaling isoprene fluxes from leaves to canopies: test cases over a boreal aspen and a mixed-species temperate forest. Journal of Applied Meteorology 38:885-898. https://doi.org/10.1175/1520-0450(1999)038<0885:SIFFLT>2.0.CO;2

Bartoń K (2020) MuMIn: Multi-Model Inference. R package version 1.43.17. https://CRAN.R-project.org/package=MuMIn

Blake RS, Monks PS, Ellis AM (2009) Proton-transfer reaction mass spectrometry. Chemical Reviews 109:861–896. https://doi.org/10.1021/cr800364q

Bohrer G, Katul GG, Walko RL, Avissar R (2009) Exploring the effects of microscale structural heterogeneity of forest canopies using large-eddy simulations. Boundary-Layer Meteorology 132:351-382. https://doi.org/10.1007/s10546-009-9404-4

Brzostek ER, Dragoni D, Brown ZA, Phillips RP (2015) Mycorrhizal type determines the magnitude and direction of root-induced changes in decomposition in a temperate forest. New Phytologist 206:1274–1282. https://doi.org/10.1111/nph.13303

Calfapietra C, Pallozzi E, Lusini I, Velikova V (2013) Modification of BVOC Emissions by Changes in Atmospheric [CO_2] and Air Pollution. In: Niinemets Ü and Monson R. (eds) Biology, Controls and Models of Tree Volatile Organic Compound Emissions. Tree Physiology, vol 5. Springer, Dordrecht. https://doi.org/10.1007/978-94-007-6606-8_10

Carter WPL (1994) Development of ozone reactivity scales for volatile organic compounds. Air

562 & Waste 44:881–899. https://doi.org/10.1080/1073161X.1994.10467290

563 Clavijo McCormick A, Gershenzon J, Unsicker SB (2014) Little peaks with big effects:
564 establishing the role of minor plant volatiles in plant-insect interactions. Plant, Cell and
565 Environment 37:1836–1844. https://doi.org/10.1111/pce.12357

566 Cleveland CC, Yavitt JB (1997) Consumption of atmospheric isoprene in soil. Geophysical
567 Research Letters 24:2379–2382. https://doi.org/10.1029/97GL02451

568 Denmead OT, Bradley EF (1985) Flux-gradient relationships in a forest canopy. In: The Forest-
569 Atmosphere Interaction (Hutchinson, BA and Hicks, BB, eds.). Dordrecht: D. Reidel
570 Publishing Co., pp. 421–442. https://doi.org/10.1007/978-94-009-5305-5_27

571 Eller ASD, Harley P, Monson RK (2013) Potential contribution of exposed resin to ecosystem
572 emissions of monoterpenes. Atmospheric Environment 77:440–444.
573 https://doi.org/10.1016/j.atmosenv.2013.05.028

574 Ellis AM, Mayhew CA (2013) Proton Transfer Reaction Mass Spectrometry: Principles and
575 Applications. John Wiley & Sons

576 Faiola CL, Vanderschelden GS, Wen M, Elloy FC, Cobos DR, Watts RJ, Jobson BT, VanReken
577 TM (2014) SOA formation potential of emissions from soil and leaf litter. Environmental
578 Science & Technology 48:938–946. https://doi.org/10.1021/es4040045

579 Fall R, Monson RK (1992) Isoprene emission rate and intercellular isoprene concentration as
580 influenced by stomatal distribution and conductance. Plant Physiology 100:987–992.
581 https://doi.org/10.1104/pp.100.2.987

582 Finnigan JJ (1985) Turbulent transport in flexible plant canopies. In: The Forest-Atmosphere
583 Interaction (Hutchinson, BA and Hicks, BB, eds.). Dordrecht: D. Reidel Publishing Co., pp.
584 421–442. https://doi.org/10.1007/978-94-009-5305-5_28

585 Freire LS, Gerken T, Ruiz-Plancarte J, Wei D, Fuentes JD, Katul GG, Dias NL, Acevedo OC,
586 Chamecki M (2017) Turbulent mixing and removal of ozone within an Amazon rainforest
587 canopy. Journal of Geophysical Research: Atmospheres 122:2791–2811.
588 https://doi.org/10.1002/2016JD026009

589 Friedlingstein P, Jones MW, O'Sullivan M, Andrew RM, Hauck J, Peters GP, Peters W, Pongratz
590 J, Sitch S, Le Quéré, Bakker DCE, Canadell JG, Ciais P, Jackson RB, Anthoni P, Barbero L,
591 Bastos A, Bastrikov V, Becker M, Bopp L, Buitenhuis E, Chandra N, Chevallier F, Chini LP,
592 Currie KI, Feely RA, Gehlen M, Gilfillan D, Gkritzalis T, Goll DS, Gruber N, Gutekunst S,
593 Harris I, Haverd V, Houghton RA, Hurtt G, Ilyina T, Jain A, Joetzjer E, Kaplan JO, Kato E,
594 Klein Goldewijk K, Korsbakken JI, Landschützer P, Lauvset SK, Levèvre N, Lenton A,
595 Lienert S, Lombardozzi D, Marland G, McGuire PC, Melton JR, Metzl N, Munro DR, Nabel
596 JEMS, Nakaoka S-I, Neill C, Omar AM, Ono T, Peregon A, Pierrot D, Poulter B, Rehder G,
597 Resplandy L, Robertson E, Rödenbeck C, Séférian R, Schwinger J, Smith N, Tans PP, Tian
598 H, Tilbrook B, Tubiello FN, van der Werf GR, Wiltshire AJ, Zaehle S (2019) Global carbon
599 budget 2019. Earth System Science Data 11:1783–1838. https://doi.org/10.5194/essd-11-
600 1783-2019

601 Fuentes JD, Chamecki M, dos Santos RMN, von Randow C, Stoy PC, Katul G, Fitzjarrald D,
602 Manzi A, Gerken T, Trowbridge A, Friere LS, Ruiz-Plancarte J, Maia JMF, Tóta J, Dias N,
603 Fisch G, Schumacher C, Acevedo O, Mercer JR, Yañez-Serrano AM (2016) Linking

meteorology, turbulence, and air chemistry in the Amazon Rain Forest. Bulletin of the American Meteorological Society 97:2329–2342. https://doi.org/10.1175/BAMS-D-15-00152.1

Fuentes JD, Lerdau M, Atkinson R, Baldocchi D, Bottenheim JW, Ciccoli P, Lamb B, Geron C, Gu L, Guenther A, Sharkey TD, Stockwell W (2000) Biogenic hydrocarbons in the atmospheric boundary layer: A review. Bulletin of the American Meteorological Society 81:1537–1575. https://doi.org/10.1175/1520-0477(2000)081<1537:BHITAB>2.3.CO;2

Fuentes JD, Wang D, Bowling DR, Potosnak M, Monson RK, Goliff WS, Stockwell WR (2007) Biogenic hydrocarbon chemistry within and above a mixed deciduous forest. Journal of Atmospheric Chemistry 56:165–185. htpps://doi.org/ 10.1007/s10874-006-9048-4

Galbally IE, Kirstine W (2002) The production of methanol by flowering plants and the global cycle of methanol. Journal of Atmospheric Chemistry, 43:195–229. https://doi.org/10.1023/A:1020684815474

Geron CD, Guenther AB, Pierce TE (1994) An improved model for estimating emissions of volatile organic compounds from forests in the eastern United States. Journal of Geophysical Research: Atmospheres 99:12773-12791. https://doi.org/10.1029/94JD00246

Goldstein AH, Goulden ML, Munger JW, Wofsy SC, Geron CD (1998) Seasonal course of isoprene emissions from a midlatitude deciduous forest. Journal of Geophysical Research: Atmospheres 103: 31045-31056. https://doi.org/10.1029/98JD02708

Goldstein AH, Galbally IE (2007) Known and unknown organic constituents in the Earth's atmosphere. Environmental Science & Technology 41:1514–1521.

https://doi.org/10.1021/es072476p

Gouw J de, Warneke C (2007) Measurements of volatile organic compounds in the Earth's atmosphere using proton-transfer-reaction mass spectrometry. Mass Spectrometry Reviews 26:223–257. https://doi.org/10.1002/mas.20119

Gray CM, Monson RK, Fierer N (2010) Emissions of volatile organic compounds during the decomposition of plant litter. Journal of Geophysical Research: Biogeosciences 115: G03015. https://doi.org/10.1029/2010JG001291

Gray CM, Monson RK, Fierer N (2014) Biotic and abiotic controls on biogenic volatile organic compound fluxes from a subalpine forest floor. Journal of Geophysical Research: Biogeosciences 119:547–556. https://doi.org/10.1002/2013JG002575

Guenther A, Zimmerman P, Klinger L, Greenberg J, Ennis C, Davis K, Pollock W, Westberg H, Allwine G, Geron C (1996) Estimates of regional natural volatile organic compound fluxes from enclosure and ambient measurements. Journal of Geophysical Research: Atmospheres 101:1345-1359. https://doi.org/10.1029/95JD03006

Guenther A (2015) Bidirectional exchange of volatile organic compounds. In: Massad RS, Loubet B (eds) Review and Integration of Biosphere-Atmosphere Modelling of Reactive Trace Gases and Volatile Aerosols. Springer, Dordrecht. https://doi.org/10.1007/978-94-017-7285-3_4

Guenther A (1997) Seasonal and spatial variations in natural volatile organic compound emissions. Ecological Applications 7:34–45. https://doi.org/10.1890/1051-0761(1997)007[0034:SASVIN]2.0.CO;2

Guenther AB, Jiang X, Heald CL, Sakulyanontvittaya T, Duhl T, Emmons LK, Wang X (2012) The Model of Emissions of Gases and Aerosols from Nature version 2.1 (MEGAN2.1): an extended and updated framework for modeling biogenic emissions. Geoscientific Model Development 5:1471–1492. https://doi.org/10.5194/gmd-5-1471-2012

Guenther A, Karl T, Harley P, Wiedinmyer C, Palmer PI, Geron C (2006) Estimates of global terrestrial isoprene emissions using MEGAN (Model of Emissions of Gases and Aerosols from Nature). Atmospheric Chemistry and Physics 3181–3210. https://doi.org/10.5194/acp-6-3181-2006

Guenther A, Zimmerman P, Wildermuth M (1993) Natural volatile organic compound emission rate estimates for United States woodland landscapes. Atmospheric Environment 28:1197-1210. https://doi.org/10.1016/1352-2310(94)90297-6

Grinspoon J, Bowman WD, Fall R (1993) Delayed onset of isoprene emission in developing velvet bean (*Mucuna* sp.) leaves. Plant Physiology 97:170-174. https://doi.org/10.1104/pp.97.1.170

Hantson S, Knorr W, Schurgers G, Pugh TAM, Arneth A (2017) Global isoprene and monoterpene emissions under changing climate, vegetation, CO_2 and land use. Atmospheric Environment 155:35–45. https://doi.org/10.1016/j.atmosenv.2017.02.010

Harley P, Greenberg J, Niinemets U, Guenther A (2007) Environmental controls over methanol emission from leaves. Biogeosciences 4: 1083-1099. https://doi.org/10.5194/bg-4-1083-2007

Holopainen JK, Blande JD (2012) Molecular plant volatile communication. In: López-Larrea C. (ed) Sensing in Nature. Advances in Experimental Medicine and Biology, vol 739. pp. 17-31. Springer, New York, NY. https://doi.org/10.1007/978-1-4614-1704-0_2

666 Holzinger R, Lee A, McKay M, Goldstein AH (2006) Seasonal variability of monoterpene
667 emission factors for a ponderosa pine plantation in California. Atmospheric Chemistry and
668 Physics 6:1267-1274. https://doi.org/10.5194/acp-6-1267-2006

669 Insam H, Seewald MSA (2010) Volatile organic compounds (VOCs) in soils. Biology and Fertility
670 of Soils 46:199–213. https://doi.org/10.1007/s00374-010-0442-3

671 Isebrands JG, Guenther AB, Harley P, Helmig D, Klinger L, Vierling L, Zimmerman P, Geron C
672 (1999) Volatile organic compound emission rates from mixed deciduous and coniferous
673 forests in Northern Wisconsin, USA. Atmospheric Environment 33:2527-2536.
674 https://doi.org/10.1016/S1352-2310(98)00250-7

675 Isidorov V, Jdanova M (2002) Volatile organic compounds from leaves litter. Chemosphere
676 48:975–979. https://doi.org/10.1016/S0045-6535(02)00074-7

677 Jin M, Liang S (2006) An improved land surface emissivity parameter for land surface models
678 using global remote sensing observations. Journal of Climate 19:2867–2881.
679 https://doi.org/10.1175/JCLI3720.1

680 Junker RR, Tholl D (2013) Volatile organic compound mediated interactions at the plant-microbe
681 interface. Journal of Chemical Ecology 39:810–825. https://doi.org/10.1007/s10886-013-
682 0325-9

683 Kaharabata SK, Schuepp PH, Fuentes JD (1999) Source footprint considerations in the
684 determination of volatile organic compound fluxes from forest canopies. Journal of Applied
685 Meteorology 38:878–884. https://doi.org/10.1175/1520-
686 0450(1999)038<0878:SFCITD>2.0.CO;2

687 Karl T, Curtis AJ, Rosenstiel TN, Monson RK, Fall R (2002) Transient releases of acetaldehyde
688 from tree leaves - products of a pyruvate overflow mechanism? Plant, Cell and Environment
689 25:1121–1131. https://doi.org/10.1046/j.1365-3040.2002.00889.x

690 Katul GG, Albertson J (1999) Low Dimensional Turbulent Transport Mechanics Near the Forest-
691 Atmosphere Interface. In: Müller P., Vidakovic B. (eds) Bayesian Inference in Wavelet-
692 Based Models. Lecture Notes in Statistics, pp. 361-380. vol 141. Springer, New York, NY.
693 https://doi.org/10.1007/978-1-4612-0567-8_22

694 Kreuzwieser J., Rennenberg H. (2013) Flooding-Driven Emissions from Trees. In: Niinemets Ü,
695 Monson R (eds) Biology, Controls and Models of Tree Volatile Organic Compound
696 Emissions. Tree Physiology, vol 5. Springer, Dordrecht. https://doi.org/10.1007/978-94-007-
697 6606-8_9

698 Kulmala M, Nieminen T, Chellapermal R, Makkonen R, Bäck J, Kerminen VM (2013) Climate
699 feedbacks linking the increasing atmospheric CO_2 concentration, BVOC emissions, aerosols
700 and clouds in forest ecosystems. In: Niinemets Ü, Monson R (eds) Biology, Controls and
701 Models of Tree Volatile Organic Compound Emissions. Tree Physiology, vol 5. Springer,
702 Dordrecht. https://doi.org/10.1007/978-94-007-6606-8_17

703 Leff JW, Fierer N (2008) Volatile organic compound (VOC) emissions from soil and litter
704 samples. Soil Biology and Biochemistry 40:1629–1636.
705 https://doi.org/10.1016/j.soilbio.2008.01.018

706 Laffineur Q, Aubinet M, Schoon N, Amelynck C, Muller JF, Dewulf J, Van Langenhove H, Steppe
707 K, Heinesch B (2012) Abiotic and biotic control of methanol exchanges in a temperate mixed

forest. Atmospheric Chemistry and Physics 12:577-590. https://doi.org/10.5194/acp-12-577-2012

Levy S, Staehelin LA (1992) Synthesis, assembly and function of plant cell wall macromolecules. Current Opinion in Cell Biology 4: 856-862. https://doi.org/10.1016/0955-0674(92)90111-O

MacDonald RC, Fall R (1993a) Acetone emission from conifer buds. Phytochemistry 34:991–994. https://doi.org/10.1016/S0031-9422(00)90700-3

MacDonald RC, Fall R (1993b) Detection of substantial emissions of methanol from plants to the atmosphere. Atmospheric Environment 27A:1709-1713. https://doi.org/10.1016/0960-1686(93)90233-O

Mäki M, Aalto J, Hellén H, Philatie M, Bäck J (2019) Interannual and seasonal dynamics of volatile organic compound fluxes from the boreal forest floor. Frontiers in Plant Science 10:191. https://doi.org/10.3389/fpls.2019.00191

McBride SG, Choudoir M, Fierer N, Strickland M (2020) Volatile organic compounds from leaf litter decomposition alter soil microbial communities and carbon dynamics. Ecology 101: e03130. https://doi.org/10.1002/ecy.3130

McKinney KA, Lee BH, Vasta A, Pho TV, Munger JW (2011) Emissions of isoprenoids and oxygenated biogenic volatile organic compounds from a New England mixed forest. Atmospheric Chemistry and Physics 11:4807-4831. https://doi.org/10.5194/acp-11-4807-2011

Menke, W (2018) Geophysical data analysis: Discrete inverse theory. Academic press. Cambridge,

728 MA, 330 pp

729 Monson RK, Baldocchi DD (2014) Terrestrial Ecosystem-Atmosphere Interactions. Cambridge
730 University Press, Cambridge, 507 pp

731 Monson RK, Grote R, Niinemets U, Schnitzler J-P (2012) Modeling the isoprene emission rate
732 from leaves. New Phytologist 195:541–559. https://doi.org/10.1111/j.1469-
733 8137.2012.04204.x

734 Monson RK, Harley PC, Litvak M, Wildermuth M, Guenther A, Zimmerman, Fall R (1994)
735 Environmental and developmental controls over the seasonal pattern of isoprene emission
736 from aspen leaves. Oecologia 99:260-270. https://doi.org/10.1007/BF00627738

737 Monson RK, Lerdau MT, Sharkey TD, et al (1995) Biological aspects of constructing volatile
738 organic compound emission inventories. Atmospheric Environment 29:2989–3002.
739 https://doi.org/10.1016/1352-2310(94)00360-W

740 Moon Z, Fuentes JD, Staebler RM (2020) Impacts of spectrally resolved irradiance on photolysis
741 frequency calculations within a forest canopy. Agricultural and Forest Meteorology 291:
742 108012. https://doi.org/10.1016/j.agrformet.2020.108012

743 Nemecek-Marshall M, MacDonald RC, Franzen JL, Wojciechowski C, Fall R (1995) Methanol
744 emission from leaves: Enzymatic detection of gas-phase methanol and relation of methanol
745 fluxes to stomatal conductance and leaf development. Plant Physiology 108: 1359-1368.
746 https://doi.org/10.1104/pp.108.4.1359

747 Niinemets Ü, Ciccioli P, Noe SM, Reichstein M (2013) Scaling BVOC emissions from leaf to

748 canopy and landscape: How different Are predictions based on contrasting emission
749 algorithms? In: Niinemets Ü, Monson R (eds) Biology, Controls and Models of Tree Volatile
750 Organic Compound Emissions. Tree Physiology, vol 5. Springer, Dordrecht.
751 https://doi.org/10.1007/978-94-007-6606-8_13

752 Niinemets Ü, Fares S, Harley P, Jardine KJ (2014) Bidirectional exchange of biogenic volatiles
753 with vegetation: emission sources, reactions, breakdown and deposition. Plant, Cell and
754 Environment 37:1790–1809. https://doi.org/10.1111/pce.12322

755 Novick KA, Ficklin DL, Stoy PC, Williams CA, Bohrer G, Oishi AC, Papuga SA, Blanken PD,
756 Noormets A, Sulman BM, Scott RL, Wang L, Phillips RP (2016) The increasing importance
757 of atmospheric demand for ecosystem water and carbon fluxes. Nature Climate Change
758 6:1023–1027. https://doi.org/10.1038/nclimate3114

759 Novick KA, Phillips RP (1999-) AmeriFlux US-MMS Morgan Monroe State Forest, Dataset.
760 https://doi.org/10.17190/AMF/1246080

761 Oliphant AJ, Rose W, Schmid H-P, Grimmond S (2006) Observations of canopy light penetration
762 and net ecosystem exchange of CO_2 under different sky conditions in a mid-western mixed
763 deciduous forest. In: Proceedings of the 27th Conference on Agricultural and Forest
764 Meteorology. American Meteorological Society

765 Oliphant AJ, Stoy PC (2018) An evaluation of semiempirical models for partitioning
766 photosynthetically active radiation into diffuse and direct beam components. Journal of
767 Geophysical Research: Biogeosciences 123:889–901. https://doi.org/10.1002/2017JG004370

768 Pau S, Detto M, Kim Y, Still CJ (2018) Tropical forest temperature thresholds for gross primary

productivity. Ecosphere 9: e02311. https://doi.org/10.1002/ecs2.2311

Peñuelas J, Llusià J (2003) BVOCs: plant defense against climate warming? Trends in Plant Science 8:105–109. https://doi.org/10.1016/S1360-1385(03)00008-6

Peñuelas J, Staudt M (2010) BVOCs and global change. Trends in Plant Science 15:133–144. https://doi.org/10.1016/j.tplants.2009.12.005

R Core Team (2020) R: A language and environment for statistical computing. R Foundation for Statistical Computing, Vienna, Austria. https://www.R-project.org/

Raupach M (1989a) Applying Lagrangian fluid mechanics to infer scalar source distributions from concentration profiles in plant canopies. Agricultural and Forest Meteorology 47:85–108. https://doi.org/10.1016/0168-1923(89)90089-0

Raupach MR (1989b) A practical Lagrangian method for relating scalar concentrations to source distributions in vegetation canopies. Quarterly Journal of the Royal Meteorological Society 115:609–632. https://doi.org/10.1002/qj.49711548710

Raupach MR (1988) Canopy transport processes. In: Steffen W.L., Denmead O.T. (eds) Flow and Transport in the Natural Environment: Advances and Applications. pp. 95-127. Springer, Berlin, Heidelberg. https://doi.org/10.1007/978-3-642-73845-6_7

Raupach MR, Shaw RH (1982) Averaging procedures for flow within vegetation canopies. Boundary-Layer Meteorology 22:79–90. https://doi.org/10.1007/BF00128057

Rinnan R, Albers C (2020) Soil uptake of volatile organic compounds: Ubiquitous and underestimated? Journal of Geophysical Research: Biogeosciences 125:e2020JG005773.

https://doi.org/10.1029/2020JG005773

Rodriguez-Iturbe I, Porporato A, Laio F, Ridolfi L (2001) Intensive or extensive use of soil moisture: Plant strategies to cope with stochastic water availability. Geophysical Research Letters 28:4495–4497. https://doi.org/10.1029/2001GL012905

Schade GW, Goldstein AH (2001) Fluxes of oxygenated volatile organic compounds from a ponderosa pine plantation. Journal of Geophysical Research: Atmospheres 106:3111–3123. https://doi.org/10.1029/2000JD900592

Schallhart S, Rantala P, Kajos MK, Aalto J, Mammarella I, Ruuskanan TM, Kulmala M (2018) Temporal variation of VOC fluxes measured with PTR-TOF above a boreal forest. Atmospheric Chemistry and Physics 18:815-832. https://doi.org/10.5194/acp-18-815-2018

Schiestl FP (2010) The evolution of floral scent and insect chemical communication. Ecology Letters 13:643–656. https://doi.org/10.1111/j.1461-0248.2010.01451.x

Schmid H, Grimmond CSB, Cropley F, Offerle B, Su H-B (2000) Measurements of CO_2 and energy fluxes over a mixed hardwood forest in the mid-western United States. Agricultural and Forest Meteorology 103:357–374. https://doi.org/10.1016/S0168-1923(00)00140-4

Sharkey TD, Singsaas EL, Lerdau MT, Geron CD (1999) Weather effects on isoprene emission capacity and applications in emissions algorithms. Ecological Applications 9:1132-1137. https://doi.org/10.1890/1051-0761(1999)009[1132:WEOIEC]2.0.CO;2

Sindelarova K, Granier C, Bouarar I, Guenther A, Tilmes S, Stavrakou T, Müller J-F, Kuhn U, Stefani P, Knorr W (2014) Global data set of biogenic VOC emissions calculated by the

809 MEGAN model over the last 30 years. Atmospheric Chemistry and Physics 14:9317–9341.
810 https://doi.org/10.5194/acp-14-9317-2014

811 Siqueira MB, Katul GG, Tanny J (2012) The effect of the screen on the mass, momentum, and
812 energy exchange rates of a uniform crop situated in an extensive screenhouse. Boundary-
813 Layer Meteorology 142:339–363. https://doi.org/10.1007/s10546-011-9682-5

814 Siqueira M, Lai C-T, Katul G (2000) Estimating scalar sources, sinks, and fluxes in a forest canopy
815 using Lagrangian, Eulerian, and hybrid inverse models. Journal of Geophysical Research:
816 Atmospheres 105:29475–29488. https://doi.org/10.1029/2000JD900543

817 Still CJ, Pau S, Edwards EJ (2014) Land surface skin temperature captures thermal environments
818 of C_3 and C_4 grasses. Global Ecology and Biogeography 23:286–296.
819 https://doi.org/10.1111/geb.12121

820 Tang J, Schurgers G, Rinnan R (2019) Process understanding of soil BVOC fluxes in natural
821 ecosystems: A review. Reviews of Geophysics 57:966–986.
822 https://doi.org/10.1029/2018RG000634

823 Trowbridge AM, Stoy PC, Phillips RP (2020) Soil biogenic volatile organic compound flux in a
824 mixed hardwood forest: Net uptake at warmer temperatures and the importance of
825 mycorrhizal associations. Journal of Geophysical Research: Biogeosciences 125:
826 e2019JG005479. https://doi.org/10.1029/2019JG005479

827 Vanhatalo A, Chan T, Aalto J, et al (2015) Tree water relations can trigger monoterpene emissions
828 from Scots pine stems during spring recovery. Biogeosciences 12:5353–5363.
829 https://doi.org/10.5194/bg-12-5353-2015

830 Wei T, Simko V, Levy M, Xie Y, Jin Y, Zemla J (2017) Package 'corrplot'. Statistician, 56: e24

831 Whelan ME, Rhew RC (2016) Reduced sulfur trace gas exchange between a seasonally dry
832 grassland and the atmosphere. Biogeochemistry 128:267–280.
833 https://doi.org/10.1007/s10533-016-0207-7

834 Yuan JS, Himanen SJ, Holopainen JK, et al (2009) Smelling global climate change: mitigation of
835 function for plant volatile organic compounds. Trends in Ecology and Evolution 24:323–331.
836 https://doi.org/10.1016/j.tree.2009.01.012

Tables

Table 1: The mean and standard deviation of studied biogenic volatile organic compound (BVOC) concentrations across all measurement heights (Figure 1) during the May 2015 study period. Values are given in parts per billion volume (ppbv). MVK: methyl vinyl ketone. MEK: methyl ethyl ketone.

Compound	Concentration (ppbv)
Formaldehyde	1.56 ± 0.60
Methanol	12.7 ± 6.5
Acetonitrile	0.23 ± 0.10
Acetaldehyde	2.30 ± 1.07
Acetone	2.97 ± 1.67
DMS	0.25 ± 0.18
Isoprene	1.32 ± 0.75
MVK	0.39 ± 0.28
MEK	0.52 ± 0.32
Benzene	0.12 ± 0.10
Toluene	0.48 ± 0.22
C8 aromatics	0.24 ± 0.15
C9 aromatics	0.69 ± 0.50
Monoterpenes	0.97 ± 0.64

Table 2: The number of times that biological and micrometeorological variables entered the linear model with the lowest AIC for models of the flux of each study biogenic volatile organic compound (BVOC, Table 1). FC: eddy covariance-measured carbon dioxide flux, H: sensible heat flux, LAI: leaf area index, LE: latent heat flux, PPFD: photosynthetically active photon flux density, $PPFD_{BC}$: below-canopy PPFD, $PPFD_{DIF}$: diffuse PPFD, SWC: soil water content, T_A: air temperature, T_{CAN}: radiometric canopy temperature, T_{FF}: radiometric forest floor temperature, T_S: soil temperature, VPD: vapor pressure deficit, WD: wind direction, WS: wind speed.

Variable	Ecosystem (of 14)	Canopy (of 14)	Forest Floor (of 14)	Total (of 42)
FC	4	4	10	18
H	13	11	8	32
LAI	12	13	14	39
LE	12	10	5	27
PPFD	12	13	10	35
$PPFD_{BC}$	0	0	0	0
$PPFD_{DIF}$	7	9	12	28
SWC	7	8	12	27
T_A	12	12	7	31
T_{CAN}	12	12	6	30
T_{FF}	10	8	5	23
T_S	1	2	12	15
VPD	14	13	14	41
WD	11	11	12	34
WS	11	11	11	33

851 **Figure Legends**

852 Figure 1: Biological and physical sources, sinks, and transport of biogenic volatile organic
853 compounds (BVOCs) in an idealized plant canopy with leaf area density (LAD, m^2 m^{-3})
854 measurements following Oliphant et al. (2006) and canopy profile measurement heights from the
855 study ecosystem: a mixed deciduous forest in the Morgan Monroe State Forest, Indiana, USA.

856

857 Figure 2: Micrometeorological conditions during the May 2015 biogenic volatile organic
858 compound canopy profile measurement campaign at the Morgan Monroe State Forest (Indiana,
859 USA) measurement tower (US-MMS). a) Air temperature measured at 46 m (T_a), soil temperature
860 measured at 10 cm depth (T_s) and above-canopy precipitation (P). b) Photosynthetically active
861 photon flux density (PPFD). c) Vapor pressure deficit (VPD). d) Wind direction (WD) measured
862 above and within the plant canopy.

863

864 Figure 3: The seasonal course of plant area index (PAI) measured using a LAI-2000 at the Morgan
865 Monroe State Forest, Indiana, USA, in the vicinity of the eddy covariance tower US-MMS for
866 2001 - 2018 with linear interpolation between measurement points. The study year 2015 is
867 indicated as a black line with black dots indicating measurements. The vertical grey bar shows the
868 time of the experimental campaign in May.

869

870 Figure 4: Time series of a) methanol, b) isoprene, and c) monoterpene concentrations as a function
871 of canopy height at Morgan Monroe State Forest (US-MMS) during the May 2015 sampling
872 period.

873

Figure 5: Average diurnal concentrations (in ppbv) of key BVOC compounds for which calibration coefficients were available (Table S1) as a function of height in the canopy during the May 2015 sampling period at the Morgan Monroe State Forest eddy covariance tower (US-MMS).

Figure 6: Modeled BVOC concentrations *versus* measurements at the eight different measurement heights for all study BVOC compounds. 1:1 lines are shown in black for reference.

Figure 7: The cumulative sum of half-hourly modeled BVOC fluxes from the ecosystem (black), plant canopy (green) and forest floor (blue) for each of the 15 study compounds during the May 2015 study period.

Figure 8: The cumulative sum of sources and sinks of the key compounds a) methanol, b) isoprene, and c) monoterpenes at different levels of the mixed hardwood forest canopy air space as estimated by the hybrid Lagrangian/Eulerian canopy modeling approach for the May 2015 study period.

Figure 9: The correlation between the ecosystem-scale flux of the three main BVOC compounds studied here – methanol, isoprene, and monoterpenes – between themselves, ecosystem-scale carbon, water, and energy fluxes, and micrometeorological variables visualized using 'corrplot' (Wei et al., 2017). Colors and ellipsoid shapes correspond to correlation coefficients, shown in the colorbar. FC: eddy covariance-measured carbon dioxide flux, H: sensible heat flux, LE: latent heat flux, LAI: leaf area index, PPFD: photosynthetically active photon flux density, $PPFD_{BC}$: below-canopy PPFD, $PPFD_{DIF}$: diffuse PPFD, SWC: soil water content, T_A: air

temperature, T_{CAN}: radiometric canopy temperature, T_{FF}: radiometric forest floor temperature, T_S: soil temperature, VPD: vapor pressure deficit, WD: wind direction, WS: wind speed.

Figures

Fig. 1

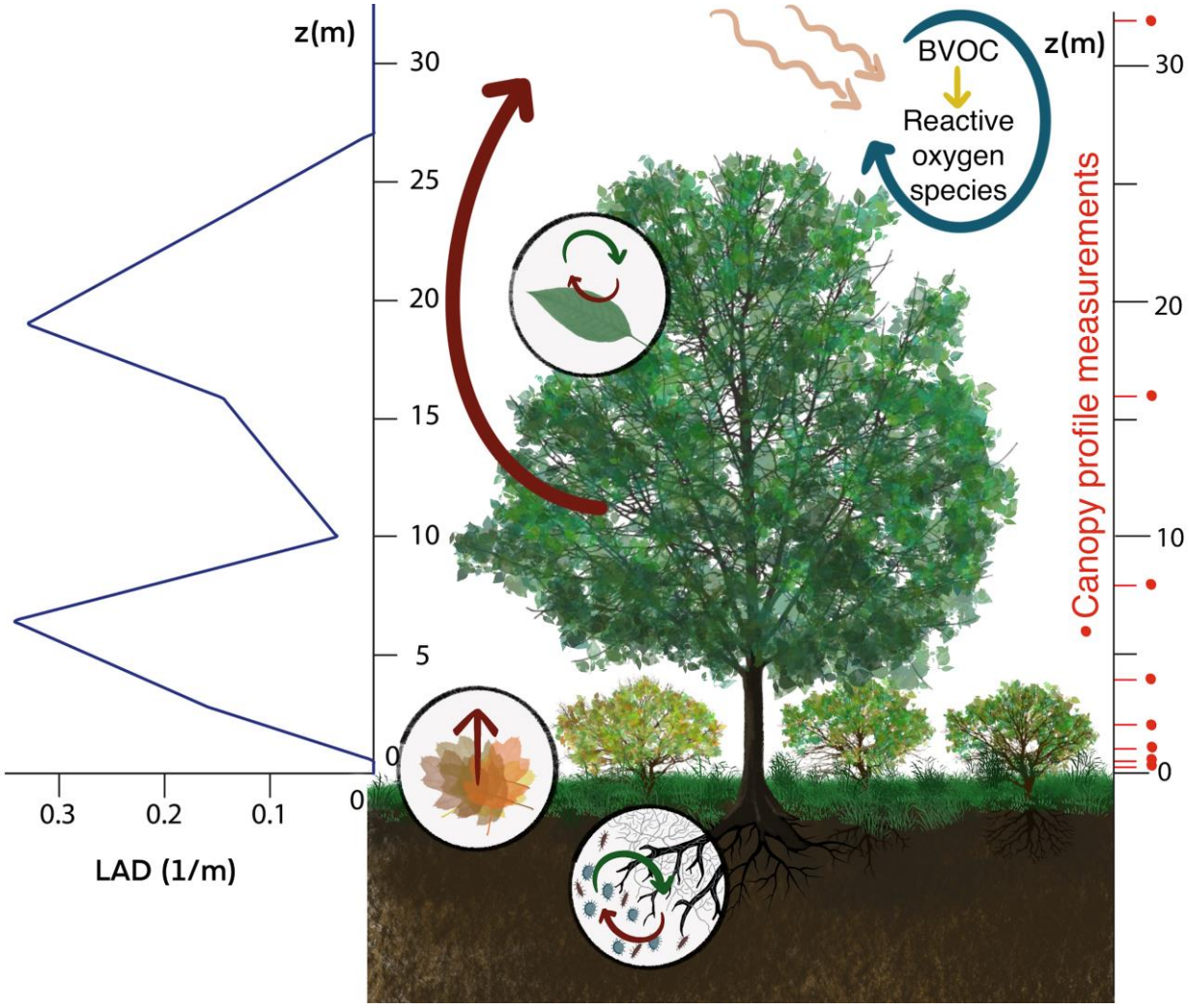

Fig. 2

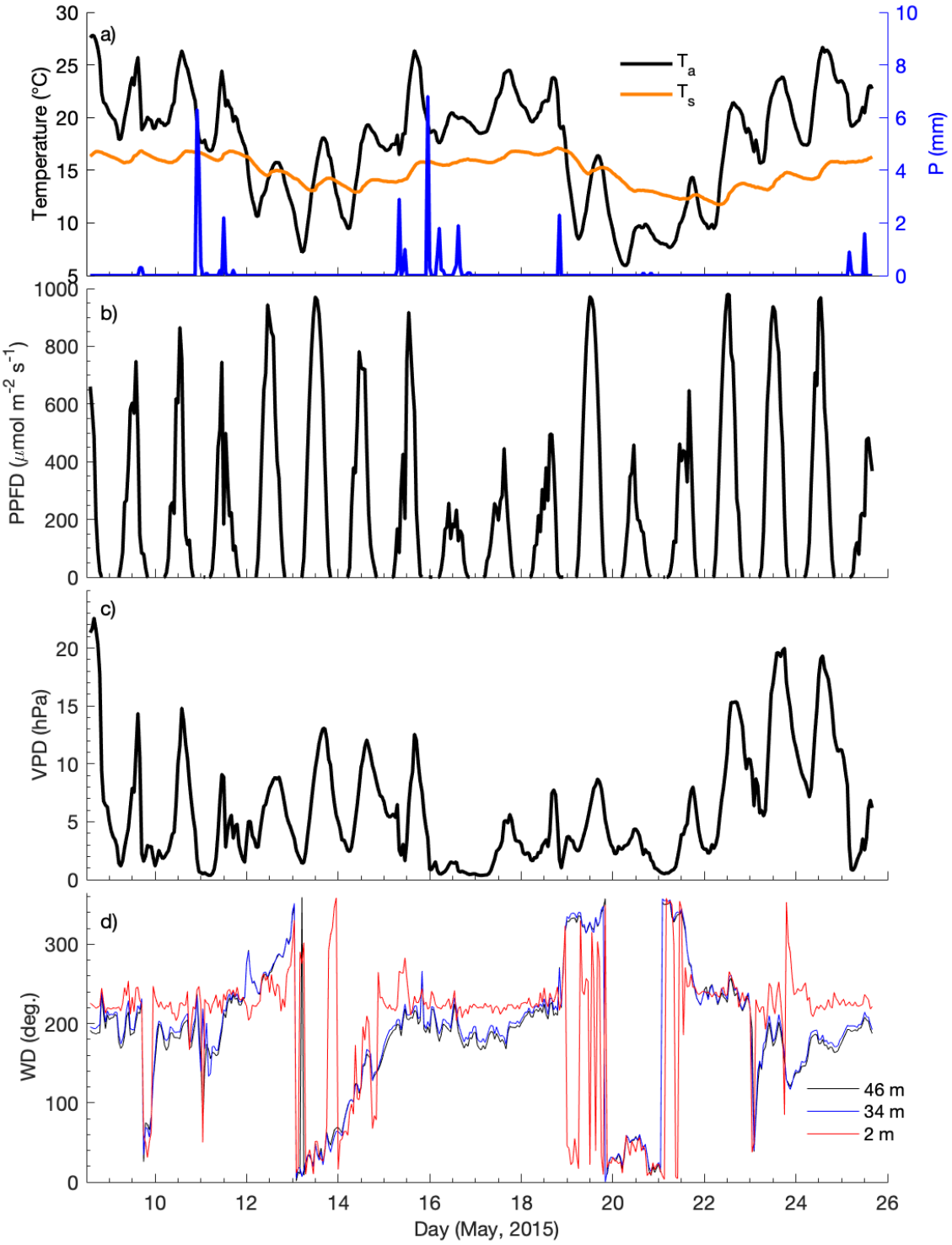
a)
b)
c)
d)
Temperature (°C)
P (mm)
T_a
T_s
PPFD (μmol m^{-2} s^{-1})
VPD (hPa)
WD (deg.)
46 m
34 m
2 m
Day (May, 2015)

Fig. 3

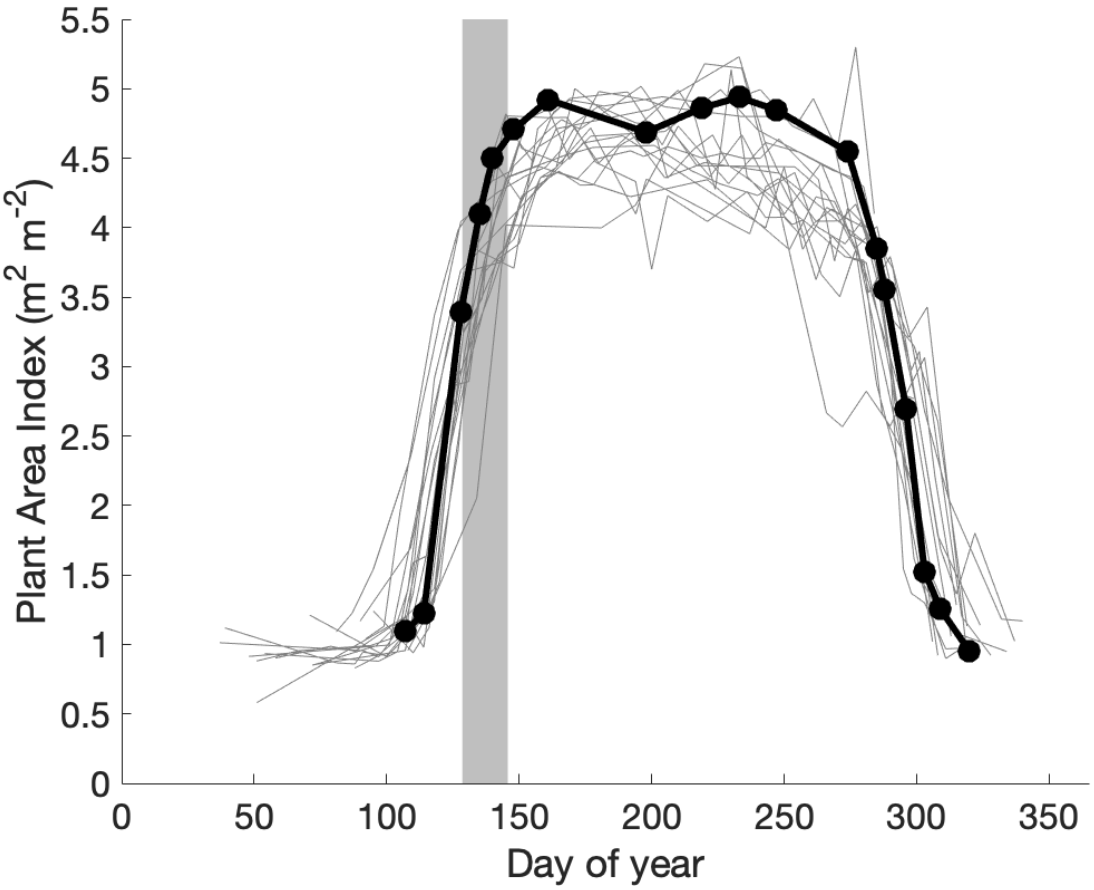
Plant Area Index (m2 m-2)
Day of year
0
0.5
1
1.5
2
2.5
3
3.5
4
4.5
5
5.5
0
50
100
150
200
250
300
350

Fig. 4

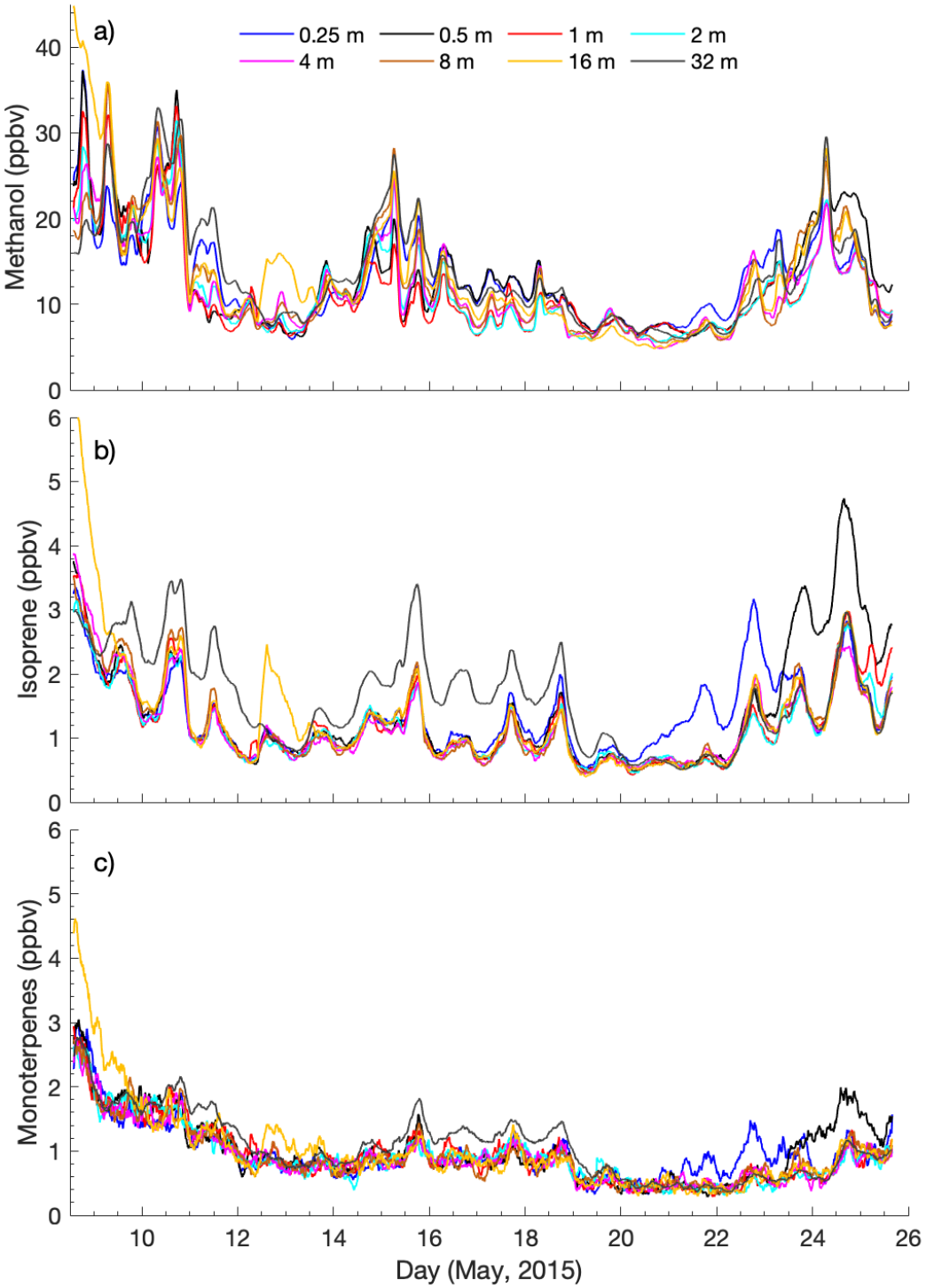
a)
0.25 m
0.5 m
1 m
2 m
4 m
8 m
16 m
32 m
Methanol (ppbv)
b)
Isoprene (ppbv)
c)
Monoterpenes (ppbv)
Day (May, 2015)

Fig. 5

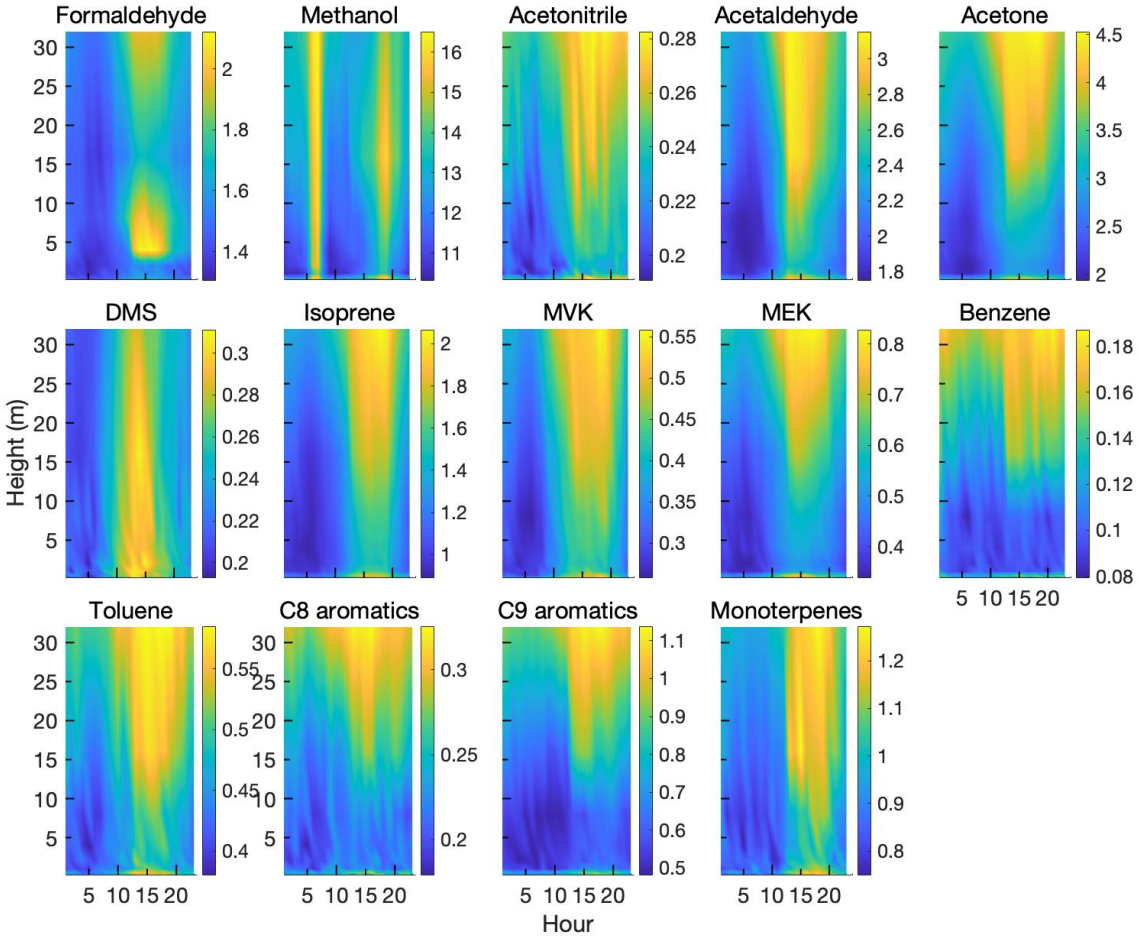
Formaldehyde
Methanol
Acetonitrile
Acetaldehyde
Acetone
DMS
Isoprene
MVK
MEK
Benzene
Toluene
C8 aromatics
C9 aromatics
Monoterpenes
Height (m)
Hour

Fig. 6

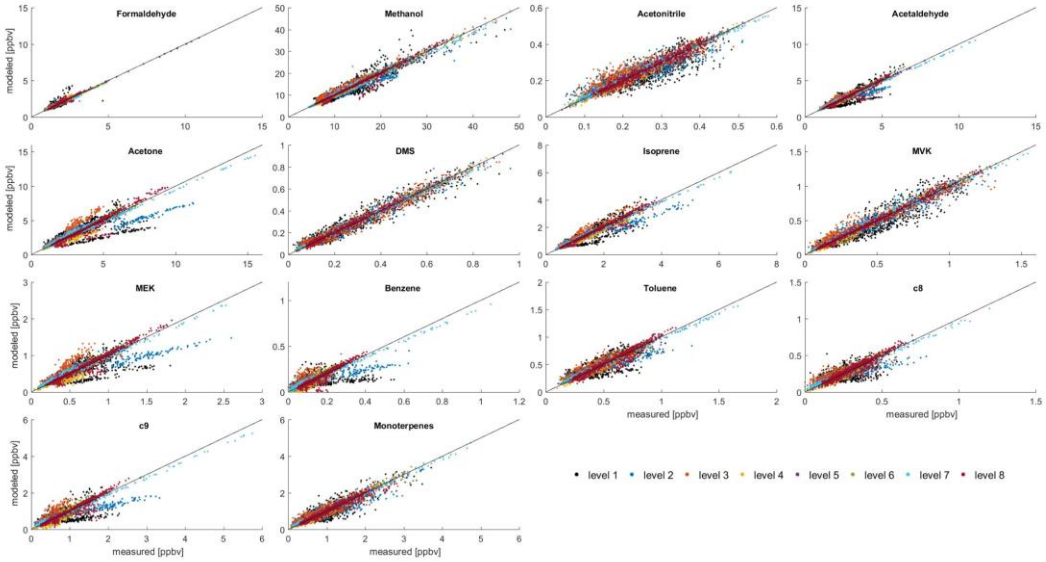
Formaldehyde
Methanol
Acetonitrile
Acetaldehyde
Acetone
DMS
Isoprene
MVK
MEK
Benzene
Toluene
c8
c9
Monoterpenes
modeled [ppbv]
measured [ppbv]
level 1
level 2
level 3
level 4
level 5
level 6
level 7
level 8

Fig. 7

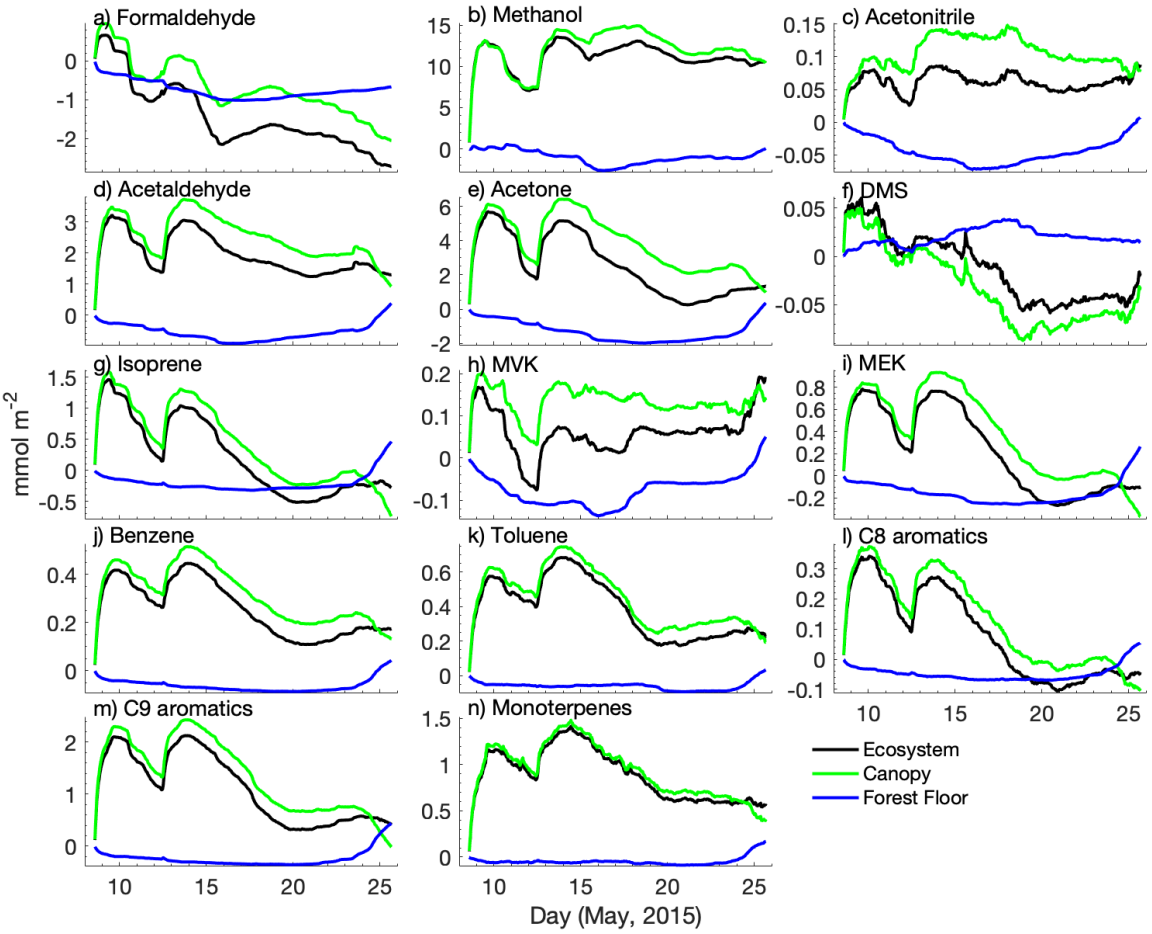
a) Formaldehyde
b) Methanol
c) Acetonitrile
d) Acetaldehyde
e) Acetone
f) DMS
g) Isoprene
h) MVK
i) MEK
j) Benzene
k) Toluene
l) C8 aromatics
m) C9 aromatics
n) Monoterpenes
mmol m-2
Day (May, 2015)
Ecosystem
Canopy
Forest Floor

Fig. 8

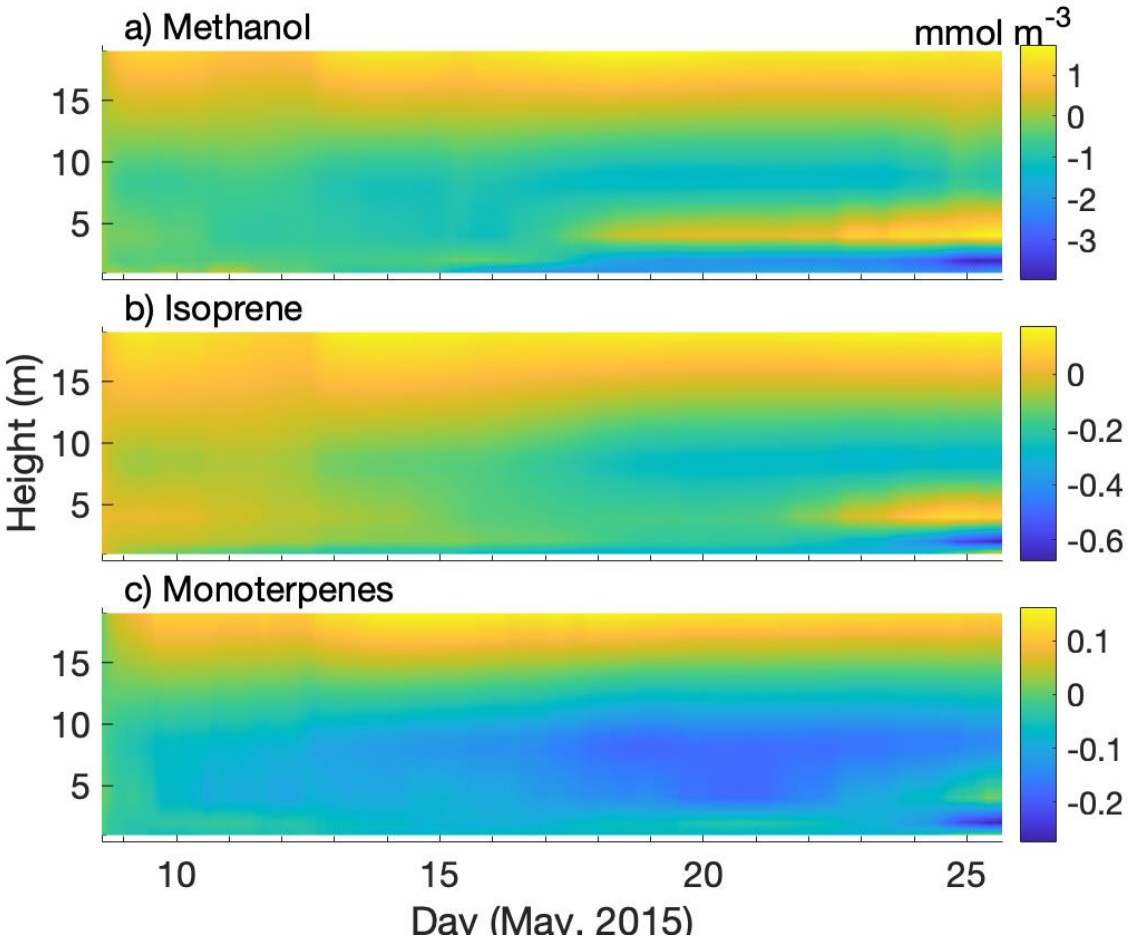
a) Methanol
mmol m-3
1
0
-1
-2
-3
b) Isoprene
0
-0.2
-0.4
-0.6
c) Monoterpenes
0.1
0
-0.1
-0.2
Height (m)
15
10
5
10
15
20
25
Day (May. 2015)

Fig. 9

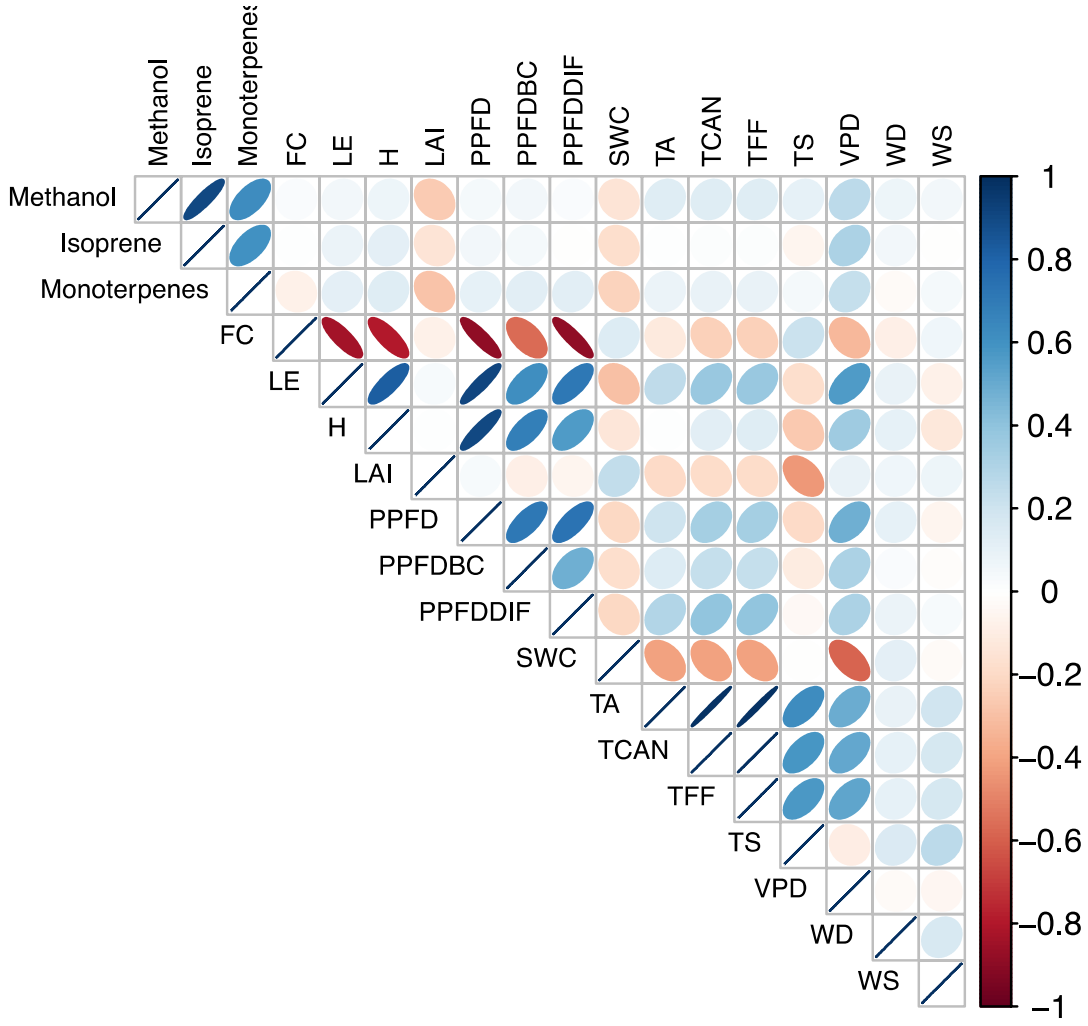
Methanol
Isoprene
Monoterpenes
FC
LE
H
LAI
PPFD
PPFDBC
PPFDDIF
SWC
TA
TCAN
TFF
TS
VPD
WD
WS
1
0.8
0.6
0.4
0.2
0
−0.2
−0.4
−0.6
−0.8
−1